



2019 AVS Prairie Chapter Symposium



Program and Abstracts

I ILLINOIS
Materials Research Laboratory
GRAINGER COLLEGE OF ENGINEERING
UNIVERSITY OF ILLINOIS



Sponsors



AVS Prairie Chapter

Program Committee

Julio Soares, *University of Illinois*
Mary Kraft, *University of Illinois*

Organizing Committee

Julio Soares (Chair), *University of Illinois*
Mary Kraft (Chair), *University of Illinois*
Julie ten Have, *University of Illinois*
Kathy Walsh, *University of Illinois*
Scott Dix, *Vacuum One*

Local Arrangements Committee

Julie ten Have, *University of Illinois*
Shannon Murray, *University of Illinois*
Doug Jeffers, *University of Illinois*

Prairie Chapter Executive Committee

Jeff Terry (Vice Chair), *Illinois Institute of Technology*
Dan Killelea (Chair), *Loyola University Chicago*
David Czaplewski (Past Chair), *Argonne National Laboratory*
Julio Soares (Treasurer), *University of Illinois*
Jessica McChesney (Secretary), *Argonne National Laboratory*
Yip-Wah Chung, *Northwestern University*
Jacob Ciszek, *Loyola University Chicago*
David Class, *Midwest Vacuum*
Scott Dix, *Vacuum One*
Nathan Guisinger, *Argonne National Laboratory*
Jiaxing Huang, *Northwestern University*
Nan Jiang, *University of Illinois at Chicago*
Alex Kandel, *University of Notre Dame*
Mary Kraft, *University of Illinois*
Paul Lyman, *University of Wisconsin*
Chris McCarthy, *Oerlikon Leybold Vacuum*
Steven Tait, *Indiana University*
Michael Trenary, *University of Illinois at Chicago*

Special Acknowledgements

University of Illinois at Urbana-Champaign AVS Student Chapter
Mauro Sardela (moderator), *University of Illinois*
Timothy Spila (moderator), *University of Illinois*

Welcome

On behalf of the AVS Prairie Chapter and the University of Illinois AVS Student Chapter, we welcome you to the 2019 AVS Prairie Chapter Symposium.

This year's symposium is a multi-topic conference, intending to instigate an exchange of ideas that goes beyond our usual collaboration circles. We have put together a very exciting program with 4 outstanding plenary talks, 8 contributed oral presentations and 43 posters on the many subjects of interest to the AVS.

We are presenting the 2019 AVS Prairie Chapter Outstanding Research Award and the 2019 AVS Prairie Chapter Early Career Award. We are fortunate to have both of this year's awardees presenting plenary talks. Dr. Jeffrey W. Elam, from Argonne National Laboratory, will present the results of his studies about the mechanisms involved in growth by atomic layer deposition in pursuit of gaining an insight into the limits of self-limitation allowing better control, successful scale-up, and the invention of new processes. Professor Ying Diao, from the University of Illinois at Urbana-Champaign, will expose to us the challenges of directing the assembly of organic electronics as inspired by the assembly processes in living organisms. In her talk, she will present new insights and strategies her group has recently developed for controlling multi-scale assembly and transformation of semiconducting molecules into the construction of organic electronics.

We also have 9 companies, which will be presenting their newest technologies at our Scientific Equipment Exhibition, supporting the symposium. We encourage you to talk to their representatives and scientists about your instrumentation questions.

Thank you for your participation and contribution to the 2019 AVS Prairie Chapter Symposium, and thanks to all who contributed to enable this outstanding program.

2019 AVS Prairie Chapter Symposium program committee

Best Student Poster Presentation Award Ceremony

Please join us at 5:45, after the last oral presentation, for a closing ceremony where we will present and celebrate this year's recipients of our Best Student Poster Presentation Award.

Wine & Cheese

5:45 p.m.
Exhibition hall



Equipment Exhibition

We have nine scientific equipment companies represented in our equipment exhibition this year. Several companies have brought some of their newest products which could include the next tool you need to complete, extend, or enrich your current project, or even start a completely new one. They have experts who can answer most questions about the equipment and many of their applications. Make sure to take some time to talk to them during the coffee breaks.

One of the highlights this year is a low-temperature Raman spectroscopy system being demonstrated by Montana Instruments. This system will be demonstrated for one week in the MRL, starting the day of the symposium.

Our exhibitors are the main sponsors of the AVS Prairie Chapter Symposia. Please make a point of thanking them for their support.

Exhibitors

Equipment exhibition opens at 10:30 and closes at 4:30
The exhibition hall is located on the second floor



Agilent

Trusted Answers

Adam Bajjalieh
adam.bajjalieh@agilent.com

ANCORP

Nancy L Hendrickson
Nancy_H@ancorp.com

HIDEN
ANALYTICAL

Mark Buckley
mark.buckley@hiddeninc.com

Kurt J. Lesker
Company

Bill Zinn
billz@lesker.com

MONTANA INSTRUMENTS[®]
COLD SCIENCE MADE SIMPLE

Craig Wall
craig.wall@montanainstruments.com

MIDWEST VACUUM

Hans Luedi
HLuedi@midwestvacuum.com

PFEIFFER  **VACUUM**

Ian Malloch and Julie Giambartolomei
JGiambartolomei@pfeiffer-vacuum.com



Chris Malocsay
chris@uccomponents.com



Scott Dix
sdix@vacuumone.com

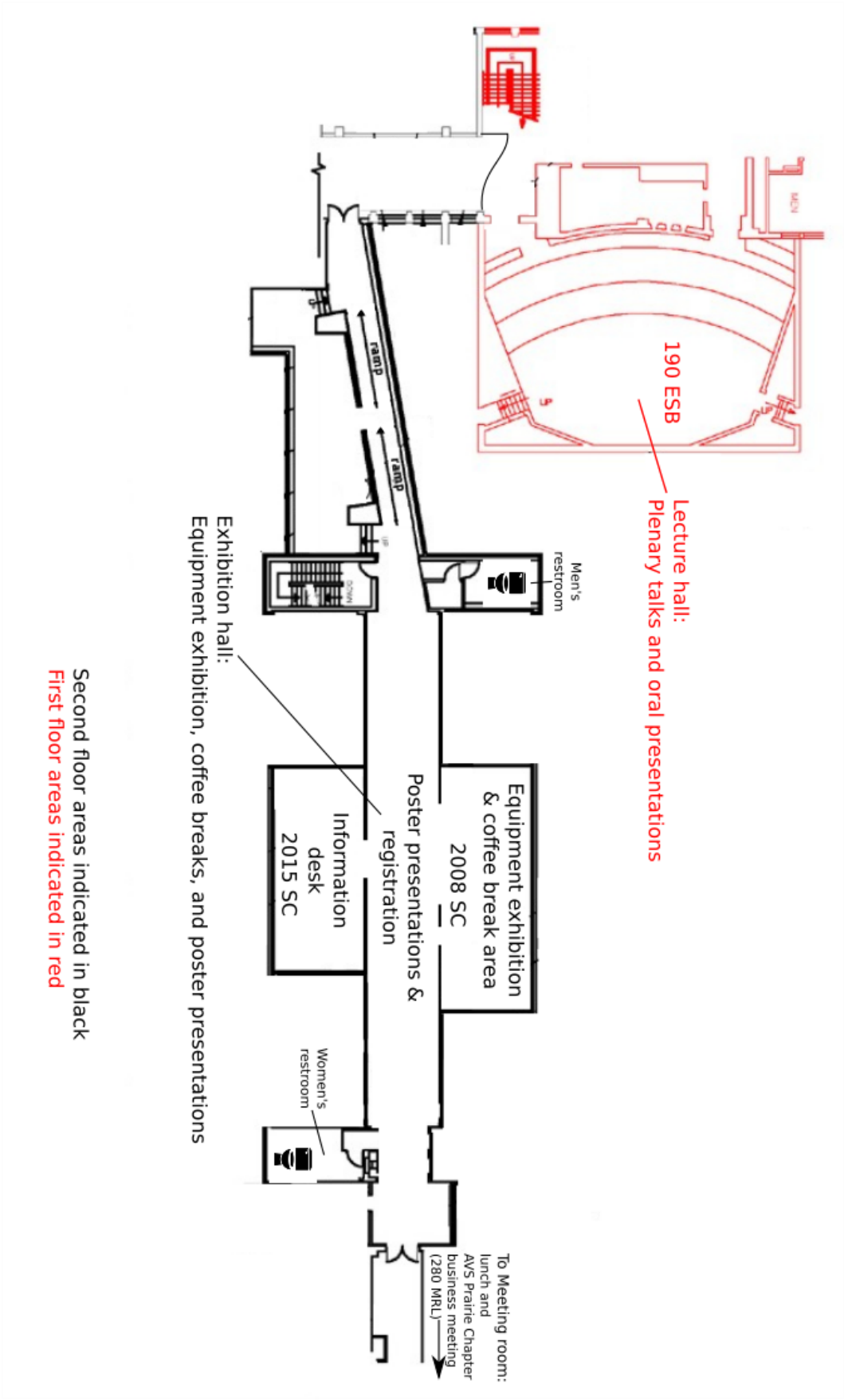
Site map



 Metered Parking

 Materials Research Laboratory

Conference rooms



Schedule summary

Time	September 5, 2019
8:30	Registration
	<i>Session A (Lecture hall) – Moderator: Mary Kraft</i>
8:45	Welcome remarks
9:15	Plenary talk AVS Prairie Chapter Early Career Research Award <u>Ying Diao</u> , University of Illinois <i>Directing assembly of organic electronics inspired by living systems</i>
10:15	<u>Cecilia M. Gentle</u> , University of Illinois - <i>Deciphering the hidden complexity of heterostructured nanocrystals</i>
10:30	<i>Coffee break and poster presentations (Exhibition hall)</i>
	<i>Session B (Lecture hall) – Moderator: Mauro Sardela</i>
11:00	Plenary talk AVS Prairie Chapter Outstanding Research Award <u>Jeffrey Elam</u> , Argonne National Laboratory <i>Elucidating the mechanisms for atomic layer growth through in situ studies</i>
12:00	<u>A. M. Boscoboinik</u> , University of Wisconsin-Milwaukee - <i>Decomposition of methyl thiolates on Cu(100)</i>
12:15	<u>Devika Choudhury</u> , Argonne National Laboratory - <i>Atomic layer deposition of HfO₂ thin films using Hf(BH₄)₄ and H₂O</i>
	<i>Lunch (Exhibition hall and Meeting room)</i>
12:30	AVS Prairie Chapter business meeting (open to all) and lunch
	<i>Session C (Lecture hall) – Moderator: Kathy Walsh</i>
2:00	Plenary talk <u>Nadya Mason</u> , University of Illinois <i>Electronic transport in strain-engineered graphene</i>
3:00	Plenary talk <u>Stephen Jacobson</u> , Indiana University Bloomington <i>Integrated micro- and nanofluidic devices for single-particle tracking of biological processes</i>
4:00	<i>Coffee break and poster presentations (Exhibition hall)</i>
	<i>Session D (Lecture hall) – Moderator: Timothy Spila</i>
4:30	<u>Steven Tait</u> , Indiana University Bloomington - <i>Tuning support interactions in metal-ligand single-site heterogeneous catalysts on powdered titania supports</i>
4:45	<u>S. Murray</u> , University of Illinois - <i>The contact-driven reduction of Mn₂O₃ to Mn₃O₄ via a propagating phase transformation front during flash sintering</i>
5:00	<u>Feifei Li</u> , Loyola University - <i>Improved interfaces by molecular surface chemical modification in organic electronics</i>
5:15	<u>Rachael G. Farber</u> , University of Chicago - <i>Nano-scale characterization of the growth and suppression behavior of niobium hydrides for next generation superconducting RF accelerators and light sources</i>
5:30	<u>Justin Bergfield</u> , Illinois State University- <i>Emergence of Fourier’s law of heat transport in quantum electron systems</i>
5:45	<i>Closing reception and poster awards ceremony</i>

List of events

- 8:00 – Poster and vendor exhibit setup starts (Exhibition hall)
- 8:30 – Registration opens (Exhibition hall)
- 8:45 – Conference talks start (Lecture hall)
- 10:30 – Equipment Exhibition and poster area opens
(Exhibition hall)
- 10:30 – Coffee break at the Equipment Exhibition
(Exhibition hall)
- 10:30 – Poster presentations and judging
(Exhibition hall)
- 11:00 – Conference talks resume (Lecture hall)
- 12:30 – Lunch served (Meeting room)
- 12:40 – AVS Prairie Chapter business meeting – open to all
(Meeting room)
- 2:00 – Conference talks resume (Lecture hall)
- 4:00 – Coffee break at the Equipment Exhibition
(Exhibition hall)
- 4:00 – Poster presentations and judging
(Exhibition hall)
- 4:30 – Conference talks resume (Lecture hall)
- 4:30 – Equipment Exhibition closes
- 5:45 – Closing reception and poster awards ceremony
(Exhibition hall)

Exhibition hall – 2008 SC and 2nd floor lobby SC

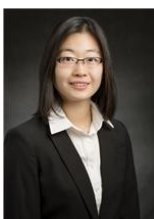
Lecture hall – 190 ESB

Meeting room – 280 MRL

Plenary talks

9:15

Directing assembly of organic electronics inspired by living systems



Ying Diao

Assistant Professor, Dow Chemical Company Faculty Scholar
Chemical and Biological Engineering, University of Illinois at Urbana-Champaign
2019 AVS Prairie Chapter Early Career Award

11:00

Elucidating the mechanisms for atomic layer growth through in situ studies



Jeffrey W. Elam

Sr. Chemist/Group Leader, Functional Coatings
Argonne National Laboratory
2019 AVS Prairie Chapter Outstanding Researcher Award

2:00

Electronic transport in strain-engineered graphene



Nadya Mason

Associate Professor
Physics, University of Illinois at Urbana-Champaign.
Director
Illinois Materials Research Science and Engineering Center

3:00

Integrated micro- and nanofluidic devices for single-particle tracking of biological processes



Stephen Jacobson

Professor, Dorothy & Edward Bair Chair
Chemistry, Indiana University Bloomington

Oral presentations

Lecture hall

Session A Moderator: Mary Kraft, University of Illinois

- 9:15 – **Plenary Talk** AVS Prairie Chapter Early Career Research Award
Ying Diao - *Directing assembly of organic electronics inspired by living systems*
- 10:15 – Cecilia M. Gentle, Yuanheng Wang, Tyler N. Haddock, Conner P. Dykstra, Renske M. van der Veen - *Deciphering the hidden complexity of heterostructured nanocrystals*

Session B Moderator: Mauro Sardela, University of Illinois

- 11:00 – **Plenary Talk** AVS Prairie Chapter Outstanding Research Award
Jeffrey Elam - *Elucidating the mechanisms for atomic layer growth through in situ studies*
- 12:00 – A. M. Boscoboinik, D. R. Olson, H. Adams, W. T. Tysoe - *Decomposition of methyl thiolates on Cu(100)*
- 12:15 – Devika Choudhury, Anil U. Mane, David Mandia, Ryan R. Langeslay, Massimiliano Delferro, Jeffrey W. Elam - *Atomic layer deposition of HfO₂ thin films using Hf(BH₄)₄ and H₂O*

Session C Moderator: Kathy Walsh, University of Illinois

- 2:00 – **Plenary Talk**
Nadya Mason - *Electronic transport in strain-engineered graphene*
- 3:00 – **Plenary Talk**
Stephen Jacobson - *Integrated micro- and nanofluidic devices for single-particle tracking of biological processes*

Session D Moderator: Timothy Spila, University of Illinois

- 4:30 – Steven Tait - *Tuning support interactions in metal-ligand single-site heterogeneous catalysts on powdered titania supports*
- 4:45 – S. Murray, T. Jensen, S. Sulekar, Y. Lin, N. Perry, D. Shoemaker - *The contact-driven reduction of Mn₂O₃ to Mn₃O₄ via a propagating phase transformation front during flash sintering*
- 5:00 – Feifei Li, Jacob W. Ciszek - *Improved interfaces by molecular surface chemical modification in organic electronics*
- 5:15 – Rachael G. Farber, Darren R. Veit, Nathan S. Sitaraman, Tomas A. Arias, and Steven J. Sibener - *Nano-scale characterization of the growth and suppression behavior of niobium hydrides for next generation superconducting RF accelerators and light sources*
- 5:30 – Justin Bergfield, Charles A. Stafford, Sosuke Inui - *Emergence of Fourier's law of heat transport in quantum electron systems*

Poster Presentations

Exhibition hall – 10:30 a.m. to 11:00 a.m. and 4:00 p.m. to 4:30 p.m.

- P1.** E. Zeynep Ayla, Daniel T. Bregante, David W. Flaherty - *Reactive surface intermediates and reaction pathways responsible for alkene oxidations with H_2O_2 over groups 4-6 substituted zeolites*
- P2.** Michelle Brann, Rebecca Thompson, Steven J. Sibener - *Morphological and temperature-dependent oxidative reactivity of propene thin films*
- P3.** Maha Alafeef, Ketan Dighe, Dipanjan Pan - *Selective detection of bacterial pathogens at single-cell resolution using metal doped carbon nanoparticles and machine learning*
- P4.** Jason Gross, Luke Hanley, Igor V. Veryovkin - *Comparing flat-top & Gaussian femtosecond laser ablation of silicon for depth profiling in mass spectrometry*
- P5.** Jason Adams, Ashwin Chemburkar, Yubing Lu, Ayman Karim, Matthew Neurock, David Flaherty - *Solvents facilitate proton-electron transfer during the direct synthesis of H_2O_2 on Pd*
- P6.** Robert Vincent Bavisotto, Wilfred T. Tysoe - *Using reflection adsorption infrared spectroscopy to investigate the surface chemistry of furfural on Pd(111)*
- P7.** Marilyn Porras-Gomez, Mijung Kim, Cecilia Leal - *Graphene-based sensing of oxygen transport through pulmonary membranes*
- P8.** Ruizhe Su, Dajla Neffati, Qiang Li, Sichuang Xue, Jaehun Cho, Jin Li, Jie Ding, Yifan Zhang, Cuncai Fan, Haiyan Wang, Yashashree Kulkarni, Xinghang Zhang - *Ultra-high strength and plasticity mediated by partial dislocations and defect networks*
- P9.** Hongping Deng, Christian J. Konopka, Tzu-Wen L. Cross, Kelly S. Swanson, Lawrence W. Dobrucki, Andrew M. Smith - *Quantitative biodistribution of multimodal macrophage-targeted nanocarrier probes by optical and nuclear imaging*
- P10.** Tomas Ricciardulli, Jason S. Adams, Coogan Thompson, Ayman Karim, David W. Flaherty - *Effect of Pd isolation on the reduction of O_2 to H_2O_2 over PdAu bimetallic nanoparticles*
- P11.** Bijal B. Patel, Dylan J. Walsh, Do Hoon Kim, Justin Kwok, Damien Guironnet, Ying Diao - *Nonequilibrium assembly of bottlebrush block copolymers for tunable nanoscale morphology and photonic properties through 3D solution printing*
- P12.** Syeda Tajin Ahmed, Deborah E. Leckband - *Investigating interactions between grafted zwitterionic polymers and proteins at nanoscale*
- P13.** Resham Rana, Wilfred T. Tysoe - *Investigation of sulfur transport and thiolate decomposition on copper*
- P14.** Kyung Sun Park, Ying Diao - *Printing flow planarized polymer backbone and induces drastic morphology transition of conjugated polymers*
- P15.** Marie E. Turano, Rachael G. Farber, Dan R. Killelea - *Oxidation reactions on Rh(111)*
- P16.** Sayantan Mahapatra, Jeremy F. Schultz, Nan Jiang - *Angstrom scale chemical analysis of intermolecular and molecule-substrate interactions by ultrahigh vacuum tip-enhanced Raman spectroscopy*

- P17.** Nathan Bennett, Justin Bergfield - *Quantum interference enhancement of the spin-thermopower*
- P18.** Muhammad Jahidul Hoque, Seok Kim, Nenad Miljkovic - *Hybrid functional surface derived from PDMS stamping*
- P19.** Jeremy Schultz, Sayantan Mahapatra, Linfei Li, Nan Jiang - *Intramolecular insights into adsorbate-substrate interactions by tip-enhanced Raman spectroscopy with angstrom-scale resolution*
- P20.** Prapti Kafle, Fengjiao Zhang, Noah B. Schorr, Kai-Yu Huang, Joaquín Rodríguez-López, Ying Diao - *Dynamic-template-directed crystallization of 2D conjugated polymer thin films and their distinct electronic properties*
- P21.** Kinsey L. Canova, Gregory S. Girolami, John R. Abelson - *Seeking superconducting Hf_{1-x}V_xB₂ (x = 0.3) by co-flow of HfB₂ and V precursors*
- P22.** David A. Turner, Catlin N. Schalk, S. Alex Kandel - *Atomic hydrogen reactions of 8-mercapto-1-octanol surfaces*
- P23.** Sarah Brown, Jeffrey Sayler, Steven J. Sibener - *Scanning tunnelling microscopy study of alkanethiolate self-assembled monolayers and their reactivity with atomic hydrogen*
- P24.** Ravi Ranjan, Michael Trenary - *Spectroscopic characterization of ethynidyne formed from acetylene on Pd(111)*
- P25.** Mohammed K. Abdel-Rahman, Michael Trenary - *Propyne hydrogenation over a Pd/Cu(111) single atom alloy catalyst studied with infrared spectroscopy*
- P26.** Zhongyao Zhang, Jennifer L. Wilson, Brian R. Kitt, David W. Flaherty - *Interlaminar shear strength enhancement of carbon fiber composite via oxygen plasma treatment*
- P27.** Angela M. Silski, Jacob P. Petersen, Jonathan Liu, S. Alex Kandel - *Molecular self-assembly of the active pharmaceutical carbamazepine on Au(111)*
- P28.** Mark Muir, Michael Trenary - *Characterization of a Pd/Ag(111) Single Atom Alloy Surface Using CO as a Probing Molecule*
- P29.** Indrajit Srivastava, Kurtis Brent, Esra Altun, Subhendu Pandit, Dipanjan Pan - *Biodegradable, photothermal-responsive, near-infrared fluorescent carbon dot probes for hypoxia detection*
- P30.** Brittney L. Gorman, Daphne Shen, Mary L. Kraft - *NanoSIMS techniques and probes for intracellular structures*
- P31.** Nate Fried, Li Wei, Maarij Syed, Marissa Tousley - *Magneto-optical characterization of magnetic nanoparticles in a liquid crystal matrix*
- P32.** Isamar Pastrana-Otero, Sayani Majumdar, Aidan Gilchrist, Brendan A. C. Harley, Mary L. Kraft - *Design, fabrication and characterization of Raman-compatible substrates that enable acquiring Raman spectra from individual cells on cell microenvironments*
- P33.** Naisong Shan, Chengtian Shen, Qiujie Zhao, Christopher M. Evans - *Structure property relationship of solid-state Li conducting network electrolyte*
- P34.** Sayani Majumdar, Isamar Pastrana-Otero, Aidan Gilchrist, Brendan A. C. Harley, Mary L. Kraft - *Profiling individual hematopoietic cells on biomaterial-based substrates with confocal Raman micro-spectroscopy*
- P35.** Haw-Wen Hsiao, Shu Li, Karin A. Dahmen, Jian-Min Zuo - *Deformation mechanism in compressed nanocrystalline ceramic nanopillars*
- P36.** Jacob P. Petersen, A.M. Silski, S.A. Corcelli, S.A. Kandel - *Surface influence in the formation of supramolecular species in two dimensions*

- P37.** Andrea Perry, Wen-Hui Cheng, Harry A. Atwater – *Photonic design of effectively transparent catalyst for higher efficiency photoelectrochemical solar fuel generators*
- P38.** A. A. Husain, M. Mitrano, S. Rubeck, M. Rak, F. Nakamura, C. Sow, Y. Maeno, P. Abbamonte – *Tuning “electronic” sound through strong electron correlations*
- P39.** Li Wei, Nate Fried, Maarij Syed – *Magneto-optical characterization of magnetic nanoparticles in aqueous solutions*
- P40.** Thomas Foulkes, Junho Oh, Nenad Miljkovic– *Impact of Nanoengineered interface design on the performance of self-assembled liquid bridge confined boiling*
- P41.** Brighton Coe, Daniel Eggena, Andrew Missel, Bailey Wilkinson, Mahua Biswas, Uttam Manna– *Dielectric nanophotonics research involving undergraduate students at Illinois State University*
- P42.** Marshall Youngblood, Mahua Biswas– *Investigation of patterned gold nanoparticles size and spacing using block copolymer lithography*
- P43.** Yulia Maximenko, V. Humbert, Z. Wang, C. Steiner, D. Iaia, A. Aishwarya, N. Mason, V. Madhavan– *In-situ Fermi level tuning of thin films during scanning tunneling microscopy studies*

ABSTRACTS

AVS Prairie Chapter Outstanding Research Award



Elucidating the mechanisms for atomic layer growth through in situ studies

Jeffrey W. Elam

Sr. Chemist/Group Leader, Functional Coatings
Argonne National Laboratory

Atomic Layer Deposition (ALD) provides exquisite control over film thickness and composition and yields excellent conformality over large areas and within nanostructures. These desirable attributes derive from self-limiting surface chemistry, and can disappear if the self-limitation is removed. Understanding the surface chemical reactions, i.e. the ALD mechanism, can provide insight into the limits of self-limitation allowing better control, successful scale up, and the invention of new processes. In situ measurements are very effective for elucidating ALD growth mechanisms. In this presentation, I will describe investigations into the growth mechanisms of ALD nanocomposite films comprised of conducting (e.g. W, Mo and Re) and insulating (e.g. Al_2O_3 , ZrO_2 and TiO_2) components using in situ measurements. These ALD nanocomposites have applications in particle detection, energy storage, and solar power. We have performed extensive in situ studies using quartz crystal microbalance (QCM), quadrupole mass spectrometry (QMS), Fourier transform infrared (FTIR) absorption spectroscopy, and current-voltage measurements. These measurements reveal unusual ALD chemistry occurring upon transitioning between the ALD processes for the two components. This results in unique reaction products that affect the properties of the films in beneficial ways. The knowledge gained from our in situ studies of the ALD nanocomposite films has helped us to overcome problems encountered when we scaled up the ALD processes to large area substrates. Beyond fundamental understanding, in situ measurements are extremely effective in ALD process development and process monitoring. I will end my talk by describing our recent work combining in situ measurements and machine learning to accelerate ALD process development.

AVS Prairie Chapter Early Career Research Award



Directing assembly of organic electronics inspired by living systems

Ying Diao

**Assistant Professor and Dow Chemical Company
Faculty Scholar**

Chemical and Biological Engineering, University of Illinois at Urbana-Champaign

Molecular assembly, crystallization and controlled phase transition have played a central role in the development of modern electronics and energy materials. Recent years, printed electronics based on semiconducting molecular systems have emerged as a new technology platform that promise to revolutionize the electronics and clean energy industry. In contrast to traditional electronic manufacturing that requires high temperature and high vacuum, these new electronic materials can be solution printed at near ambient conditions to produce flexible, light-weight, biointegrated forms at low-cost and high-throughput. However, it remains a central challenge to control the morphology of semiconducting molecular systems across length scales. The significance of this challenge lies in the order of magnitude modulations in device performance by morphology parameters across all length scales. This challenge arises from the fact that directed assembly approaches designed for conventional hard materials are far less effective for soft matters that exhibit high conformational complexity and weak, non-specific intermolecular interactions. On the other hand, biological systems have evolved to assemble complex molecular structures highly efficiently. We are eager to transfer the wisdom of living systems to developing printed electronics technologies as to enable next generation electronics for clean energy and healthcare. In this talk, we present new insights and strategies we recently developed for controlling multi-scale assembly and transformation of semiconducting molecules. We learned from living systems and designed bioinspired assembly processes, allowing molecules to put themselves together cooperatively into highly ordered structures otherwise not possible with significantly improved electronic properties. We discovered molecular design rules that impart dynamic and switchable electronic properties through the mechanism of molecular cooperativity – a mechanism ubiquitous in nature. These new solid-state properties could potentially enable new sensing and actuation mechanisms not possible before. We further developed 2D and 3D printing process to realize on-the-fly morphology control down to the molecular and nanoscale.

Plenary talk



Electronic transport in strain-engineered graphene

Nadya Mason

Associate Professor

Physics, University of Illinois at Urbana-Champaign.

Director

Illinois Materials Research Science and Engineering Center

There is wide interest in using strain-engineering to modify the physical properties of 2D materials, for both basic science and applications. Deformations of graphene, for example, can lead to the opening of band gaps, as well as the generation of pseudo-magnetic fields and novel quantum Hall states. We demonstrate how controllable, device-compatible strain patterns in graphene can be engineered by depositing graphene on corrugated substrates. We discuss several techniques for creating corrugated substrates, focusing on periodic spherical curvature patterns in the form of closely packed nanospheres. We show how the smaller nanospheres induce larger tensile strain in graphene, and explain the microscopic mechanism of this. We also present experimental results demonstrating how a nearly periodic array of underlying nanospheres creates a strain superlattice in graphene, exhibiting mini-band conductance dips and magnetic field effects that depend on the magnitude of induced strain.

Plenary talk



Integrated micro- and nanofluidic devices for single-particle tracking of biological processes

Stephen Jacobson

Professor, Dorothy & Edward Bair Chair
Chemistry, Indiana University Bloomington

We are developing integrated micro- and nanofluidic devices to study virus assembly and bacterial development at the single-particle level. Analysis of single particles provides unprecedented insight into biological processes that are often missed when a population is studied as an ensemble. For fabrication of these integrated devices, we combine focused-ion beam milling or electron-beam lithography with photolithography, wet-chemical etching, and cover plate bonding.

To characterize capsid assembly of hepatitis B virus, we are using resistive-pulse sensing as a label-free, nondestructive technique. This single-particle method permits real-time detection and has sufficient sensitivity to monitor assembly at biologically relevant concentrations and over a range of reaction conditions.

Assembly in the presence of potential antivirals and chaotropes produces a variety of particle morphologies, including normal capsids, kinetically trapped intermediates, and aberrant structures. To study development of bacteria, we have integrated nanochannel arrays into a microfluidic platform that physically trap bacteria. The nanochannels confine growth of bacteria in one dimension, and when coupled with fluorescence microscopy, these devices measure bacterial processes with improved temporal and spatial resolution. Growth and division rates, subcellular functions, epigenetic effects, and antibiotic response are easily tracked for extended periods of time and across multiple generations.

Deciphering the hidden complexity of heterostructured nanocrystals

Cecilia M. Gentle, Yuanheng Wang, Tyler N. Haddock, Conner P. Dykstra, Renske M. van der Veen

Department of Chemistry and Materials Research Laboratory
University of Illinois at Urbana-Champaign, Urbana, Illinois

Colloidal semiconductor quantum dot nanocrystals exhibit size dependent optoelectronic properties due to their quantum-confined excited states. The precise control over charge-carrier localization recombination dynamics make quantum dots interesting candidates for photovoltaics, lasers, LEDs, and biomedical imaging devices. The charge-carrier distribution and rate of recombination in nanocrystals can be further tuned by the addition of multiple components and heterointerfaces. Charge carriers can be spatially localized by selecting components with particular valance and conduction band energy offsets. Type-I heterostructures feature a nested configuration such that the band gap of one material is encompassed within the band gap of the other material. This confines the photoinduced charges exclusively within the material containing the smaller, encompassed band gap. In type-II alignment, the band energies have a staggered band alignment which results in separation of the photo-excited electrons and holes across the material interface.

ZnTe/CdSe core-shell particles have been shown to exhibit broadly tunable luminescence in the visible and near-IR region, making them suitable for fluorescence applications. Core/shell nanocrystals can be typically characterized using high resolution transmission electron microscopy (TEM). Because ZnTe and CdSe both have zinc blende crystal structures and similar atomic weights, there is no observable difference in electron diffraction and Z contrast between the core and the shell in TEM. Alloying of these two miscible structures further complicates the structure, making it more challenging to characterize the internal structure via TEM or X-ray diffraction. Our approach employs X-ray spectroscopy (XAS) methods. XAS is ideally suited for probing the internal structure of multicomponent materials because of its elemental specificity and sensitivity to local structure of the absorbing atom. The extended X-ray absorption fine structure (EXAFS) can ascertain coordination numbers, distinguish between types of scattered atoms, calculate bond lengths, and determine bond angles in the local (~ 6 Å) environment of the absorbing atom in the nanoparticle.

Here, we show that nominal ZnTe/CdSe core/shell quantum dots synthesized by standard procedures in the literature in actuality have an alloyed $\text{Zn}_x\text{Cd}_{1-x}\text{Te}$ core with a thin CdSe shell. We studied the local structure of each elemental component of these structurally complex nanoparticles by individually probing the Zn, Te, Cd, and Se X-ray absorption K-edges. Our results confirm (1) the presence of Cd-Te bonds (2) gradient alloying at the interfaces, and (3) a patchy CdSe shell. We extend our structural analysis with electronic band structure calculations and UV/vis absorption spectroscopy, demonstrating that the alloyed $\text{Zn}_x\text{Cd}_{1-x}\text{Te}$ /CdSe core/shell quantum dots exhibit a type-I band alignment, different from the predicted type-II band alignment of the intended ZnTe/CdSe core/shell quantum dots. This study highlights the power of XAS for understanding the internal structure of heterogenous nanoparticles.

Underneath the force-monitoring mechanochemical decomposition of methyl thiolates on Cu(100)

A. M. Boscoboinik, D. R. Olson, H. Adams, W. T. Tysoe

Department of Chemistry and Biochemistry
University of Wisconsin-Milwaukee, Milwaukee, Wisconsin

Improving lubricant additives and identifying how they react at surfaces is important for reducing macroscopic and microscopic friction (e.g. cars and micromachines).¹ By dosing dimethyl disulfide (DMDS) on Cu(100) a model lubricant film of methyl thiolates is produced. The aforementioned film has been considered, among other dialkyl disulfides, sufficiently reactive that they could form the basis of lubricants for the sliding copper-copper interface at room temperature.² The mechanically induced rate of a chemical reaction is described by the Bell model³ where the rate constant for a reaction under an applied stress σ is given by $k(\sigma) = k_0 \exp(\sigma \Delta V^\ddagger / k_B T)$, here k_B is the Boltzmann constant, k_0 is the reaction rate in the absence of stress, ΔV^\ddagger is known as the activation volume and T is the absolute temperature. While exponential increases in reaction rates with stress have been reported, there are currently no quantitative measurements. This is addressed by using contact-mode Atomic Force Microscopy (AFM) to measure the kinetics of mechanochemically induced C-S bond cleavage in methyl thiolates on Cu(100) in ultrahigh vacuum. The mechanochemical reaction is studied by analyzing the evolution of the topography of the surface as a function of time at various contact pressures. The experimental rate of methyl thiolate decomposition increases exponentially with stress (Fig. 1, ■) with an activation volume of $46 \pm 5 \text{ \AA}^3$, but this value does not agree quantitatively with the predictions of the Bell model (—). However, the results of DFT calculations⁴ of the energy barrier for methyl thiolate decomposition under the influence of a normal force (—) provide excellent agreement with experiment. An analysis of the calculations indicates that the effect of a normal stress is to both destabilize the initial state and to lower the energy of the transition state.

These results will enable descriptions of mechanochemical reactions to be placed on a firm theoretical footing that will ultimately enable them to be quantitatively predicted.

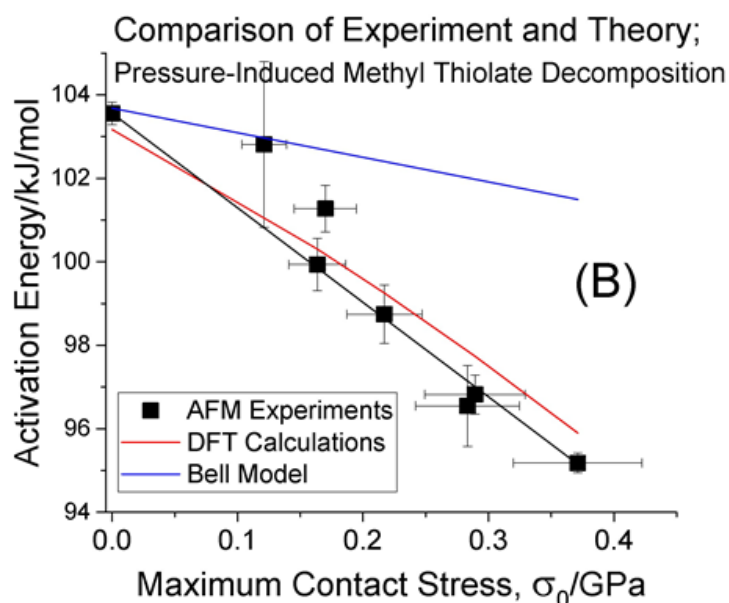


Figure 1

Comparison of experiment and theory. Reaction activation energy versus maximum contact stress, compared with the results of the Bell model (—) and those of DFT calculations (—).

¹ O.M. Braun, A.G. Naumovets, Surf. Sci. Rep. 60, 79–158 (2006)

² O. J. Furlong, B. P. Miller, Z. Li, J. Walker, L. Burkholder, W. T. Tysoe, Langmuir. 26, 21, 16375–16380 (2010)

³ G. I. Bell, Cell Biophys. 1, 133 (1979)

⁴ H. L. Adams, UWM Theses/Dissertations. 1566, 145, (2017)

Atomic layer deposition of HfO₂ thin films using Hf(BH₄)₄ and H₂O

Devika Choudhury, Anil U. Mane, David Mandia, Ryan R. Langeslay, Massimiliano Delferro,
Jeffrey W. Elam

Argonne National Laboratory
Argonne, Illinois

High dielectric constant (high-k) metal oxides and their silicates have been extensively studied as alternatives to SiO₂ for electronic and optoelectronic applications.¹ Excellent dielectric properties coupled with high thermal stability has made HfO₂ one of the most popular replacements for SiO₂ in CMOS and DRAM devices. HfO₂ thin films have been deposited using various methods including CVD, ALD, sputtering, and sol-gel techniques.² However, with the decreasing size of devices and increasing demand for ultrathin conformal films with precise thickness and composition control, ALD has emerged as the preferred method.

ALD of HfO₂ has so far been successfully implemented using different precursors. HfCl₄ and HfI₃ are two of the most commonly used Hf sources, which however require high deposition temperatures (>300°C) and generate corrosive byproducts (HCl and HI). Although alternative precursors like metalorganics or amides have also been used, the possibility of carbon contamination has restricted their use in electronic applications.³

In this work, we demonstrate the relatively low temperature ALD of HfO₂ thin films using a carbon free precursor, tetrakis(tetrahydroborato)hafnium [Hf(BH₄)₄], and H₂O. As both precursors have substantial vapor pressure at room temperature, low temperature deposition growth is possible. Self-limiting, linear growth of HfO₂ is obtained at 200°C, and experiments on the feasibility of lower temperatures deposition are underway. The refractive index of the as-grown films measured at 632 nm is found to be 1.91, which indicates the formation of HfO₂. Stronger confirmation for HfO₂ is obtained by elemental analysis using X-ray photoelectron spectroscopy (XPS). The doublet of the Hf 4f orbital electrons obtained at binding energies of 18.4 and 20.1 eV can be assigned to the Hf 4f_{7/2} and Hf 4f_{5/2} electronic states of Hf in Hf-O bonds respectively. Moreover, the O1s peak obtained observed at 531.9 eV also corresponds to formation of Hf-O bonds in the as-deposited film. XRD analysis showed the films deposited at 200°C to be amorphous, but rapid thermal annealing at 750°C for 60s yields crystalline, monoclinic HfO₂ films.

¹ E.P. Gusev, C. Cabral Jr., M. Copel, C. D'Emic and M. Gribelyuk; *Microelectronic Engineering* 69 (2003) 145–151

² K. Kukli, M. Ritala, T. Sajavaara, J. Keinonen and M. Leskela; *Thin Solid Films* 416 (2002) 72–79

³ K. Kukli, M. Ritala, J. Sundqvist, J. Aarik, J. Lu, T. Sajavaara, A. Harsta and M. Leskela, *Journal of Applied Physics*; 92 (2002) 5698-5703.

Tuning support interactions in metal-ligand single-site heterogeneous catalysts on powdered titania supports

Steven L. Tait

Department of Chemistry
Indiana University

Single-site catalysis is a field of growing interest because of the promise of atom efficiency, high selectivity, stability, and new catalytic pathways for heterogeneous catalysts. Our group investigates on-surface metal-ligand complexation to achieve high levels of selectivity with chemically uniform metal single-sites at surfaces. We have examined a variety of ligand-metal combinations on model surfaces to find systems that achieve on-surface redox complexation to form stable and chemically active metal sites. We have also assembled quasi-square planar metal-organic complexes on high surface area powdered oxides through a modified wet-impregnation method. X-ray photoelectron spectroscopy measurements demonstrate loading of metal and ligand on the surface and synchrotron-based X-ray absorption spectroscopy measurements of the coordination shell of the metal centers demonstrates single site formation rather than nanoparticle assembly. These systems are shown to be active for the catalysis of hydrosilylation reactions at a level that is competitive with current homogeneous catalysts. This presentation will report effects on metal-ligand single-site catalysts (SSCs) from modification of the defect density in titania supports. These results contribute to a better understanding of the tenability of metal-ligand SSCs through control of ligand and support.

The contact-driven reduction of Mn_2O_3 to Mn_3O_4 via a propagating phase transformation front during flash sintering

S. Murray, T. Jensen, S. Sulekar, Y. Lin, N. Perry, D. Shoemaker

Department of Materials Science and Engineering
University of Illinois at Urbana-Champaign, Urbana, Illinois

Flash sintering is a method to rapidly densify ceramics by applying an electric field at elevated temperatures. A handful of studies have applied flash sintering as a synthesis technique. For example, BiFeO_3 may be synthesized by combining and flashing Bi_2O_3 with Fe_2O_3 . This work demonstrates that reactive flash sintering can be extended to redox reactions. Additionally, we demonstrate the importance of selecting an appropriate electrode material. When Mn_2O_3 is flash sintered with Pt electrodes using suitable experimental parameters, it transforms into Mn_3O_4 via a phase transformation front that propagates from the electrodes.

When Mn_2O_3 is flashed above a threshold electric field and furnace temperature, and the flash is held for a sufficient amount of time, an orange glow progresses from one or both electrodes. Using ex-situ X-ray diffraction and Rietveld refinements, the black areas are found to be Mn_2O_3 while the glowing, orange areas are Mn_3O_4 . Therefore, the moving phase transformation front is visually apparent. Since the phase transformation can propagate from either electrode, the polarity of the electrode does not cause the initiation or propagation of the transformation. The energy needed for the endothermic phase transformation from Mn_2O_3 to Mn_3O_4 is provided by contact resistance-induced Joule heating. The conversion of Mn_2O_3 to Mn_3O_4 may occur at furnace temperatures as low as 285°C , far lower than the conventional transition temperature of 950°C . In some cases, the transformation can propagate after the flash without applying external heat from the furnace.

Selecting an appropriate electrode material is critical to produce a phase transformation since sufficient contact resistance is needed. Room temperature impedance measurements demonstrate that Pt electrodes provide substantial contact resistance while Ag electrodes do not. So, for Mn_2O_3 , Pt electrodes are needed to maximize contact resistance and cause local Joule heating to initiate the phase transformation.

Improved interfaces by molecular surface chemical modification in organic electronics

Feifei Li, Jacob W. Ciszek

Department of Chemistry and Biochemistry
Loyola University Chicago, Chicago, Illinois

Organic materials continue to find widespread adoption in optoelectronic devices, despite the fact that interfacial limitations continue to plague their effectiveness. We pioneered surface chemistry on acene thin film several years ago, specifically Diels-Alder chemical reaction on the organic semiconductor, in the hopes of alleviating many of surface issues such as adhesion, metal penetration, and electron injection barriers. Here we present findings that help elucidate the mechanism by which these solid-vapor reactions proceed for molecular thin films. A prototypical system, a vapor-solid Diels-Alder reaction of tetracene and pentacene thin-films, is used to observe the evolution of morphology features as the reaction transitions from surface to bulk. Our chemical transformations utilize an anhydride terminated self-assembled monolayers on tetracene and pentacene as the starting point. During reaction, the chemical changes cause a disruption of the surface, forming asperities. We find these surface morphology features occurs via a mechanism whereby a small amount of the adsorbate vapor condenses on the surface allowing the product to migrate to form larger aggregates. This chemistry is then applied towards improving the metal on semiconductor contact. As a demonstration of principle, a secondary reaction following the Diels-Alder chemistry is utilized to form covalent bonds linking the organic semiconductor with a deposited metal contact thereby eliminating the poor adhesion present in this system.

Nano-scale characterization of the growth and suppression behavior of niobium hydrides for next generation superconducting RF accelerators and light sources

Rachael G. Farber,¹ Darren R. Veit,¹ Nathan S. Sitaraman,² Tomas A. Arias,² Steven J. Sibener¹

¹Department of Chemistry and The James Franck Institute
University of Chicago, Chicago, Illinois

²Department of Physics
Cornell University, Ithaca, New York

Particle accelerator science and technology, while commonly associated with fundamental high-energy physics applications, is also a crucial component in biological, chemical, and industrial scientific technologies. In order to increase the accessibility and applicability of accelerator-based technologies in multiple sectors, it is imperative to develop technologies that will enable the production of a more intense particle beam at a lower price point. As such, it is essential to identify structural and chemical features that inhibit beam intensity and develop methods to suppress such surface features.

Niobium (Nb) is the current standard for superconducting radio frequency (SRF) accelerator cavities due to its ultra-low surface resistance (R_s) and high cavity quality factor (Q) at operating temperatures of ~ 2 K. It is known that SRF cavity surface composition and contaminant incorporation is directly related to Q ; hydrogen incorporation, which results in the formation of Nb hydrides, has been identified as a major source of decreased Q . There is not, however, a fundamental understanding of the growth mechanism for Nb hydrides. We have investigated Nb(100) samples infused with hydrogen using low-temperature scanning tunneling microscopy (LT-STM) and scanning tunneling spectroscopy (STS) to elucidate the nano-scale growth behavior and electronic characteristics of Nb hydrides. In addition, results from Fermi National Accelerator Laboratory have revealed the beneficial effects of nitrogen doping on SRF cavity performance. To understand the effects of nitrogen doping on Nb hydride growth, we have studied Nb(100) samples infused with both hydrogen and nitrogen using LT-STM and STS. In addition to novel experimental insight, we have collaborated with researchers at Cornell University to elucidate the complex bandgap behavior observed during STS experiments for both the hydrogen and hydrogen and nitrogen infused Nb. These preliminary DFT calculations investigating the surface local density of states (LDOS) support our experimental observations, and provide significant insight into the importance of hydrogen and nitrogen on the Nb LDOS.

Emergence of Fourier's law of heat transport in quantum electron systems

Justin Bergfield, Charles A. Stafford, Sosuke Inui

Department of Chemistry
Illinois State University, Normal, Illinois

The microscopic origins of Fourier's law of thermal transport in quantum electron systems has remained somewhat of a mystery, given that previous derivations were forced to invoke intrinsic scattering rates far exceeding those occurring in real systems. We propose an alternative hypothesis, namely, that Fourier's law emerges naturally if many quantum states participate in the transport of heat across the system. We test this hypothesis systematically in a flake junction, and show that the temperature distribution becomes nearly classical when the broadening of the individual quantum states of the flake exceeds their energetic separation. We develop a thermal resistor network model to investigate the scaling of the sample and contact thermal resistances, and show that the latter is consistent with classical thermal transport theory in the limit of large level broadening.

ABSTRACTS

Poster presentations

Reactive surface intermediates and reaction pathways responsible for alkene oxidations with H₂O₂ over groups 4-6 substituted zeolites

E. Zeynep Ayla, Daniel T. Bregante, David W. Flaherty

Department of Chemical and Biomolecular Engineering
University of Illinois at Urbana-Champaign, Urbana, Illinois

Epoxides are important precursors for the production of several commodity chemicals. The chlorohydrin and organic-hydroperoxide epoxidation processes create large amounts of toxic and caustic co-products (e.g., aqueous chlorine, HOCl, organic acids) that must be chemically remediated prior to disposal. Hydrogen peroxide (H₂O₂) is an environmentally-friendly alternative that can be used as an oxidant and yields only water as a by-product. We aim to develop structure-function relationships among groups 4-6 transition metals (i.e., Ti, Nb, and W) in zeolite frameworks which activate H₂O₂ for the oxidation of alkenes. While groups 4 and 5 metal heterogeneous catalysts are known to selectively epoxidize alkenes,¹ less is known about reaction pathways and reactive intermediates formed during reactions of H₂O₂ with group 6 atoms in zeolite BEA. This information may help to explain the reasons for significant differences between the types of products formed over these similarly structured catalysts.

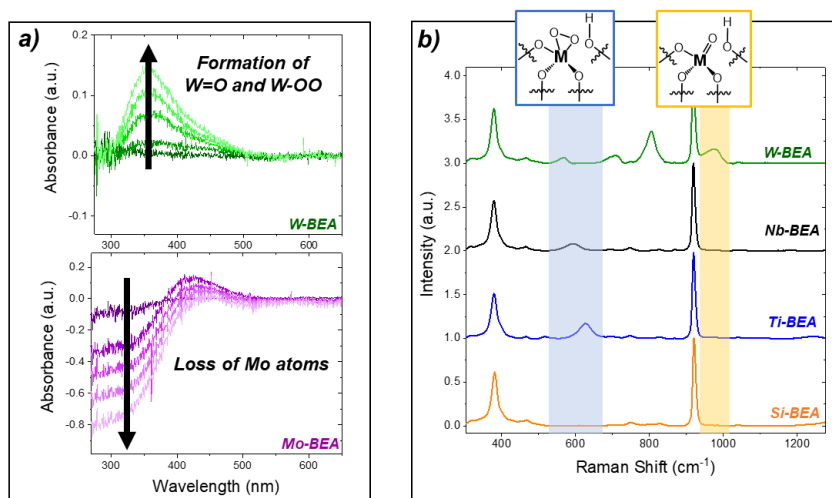


Figure 1

(a) UV-Vis spectra taken while flowing 0.01 M H₂O₂ in CH₃CN, 313 K,

(b) Raman difference spectra of M-BEA taken following addition of 0.01 M H₂O₂, (CH₃CN solvent, 442 nm laser, 20 mW, 40 accumulations, 0.1 s⁻¹ exposure time, 313 K)

Group 6 metals are known to leach significantly from heterogeneous supports and have low selectivity to the epoxide when incorporated into zeolite BEA. In situ UV-Vis and Raman experiments under reaction conditions show that greater than 90% of Mo atoms leach from the BEA framework, while W remains largely stable, making W a comparable group 6 metal to Ti and Nb when incorporated into BEA (Figure 1a). Furthermore, in situ UV-Vis experiments and the isomeric structure of the cis-stilbene epoxidation product support that groups 4 and 5 M-BEA react through metal hydroperoxo (M-OOH) and peroxo (M-O₂) moieties, respectively. Raman spectra of M-BEA collected in situ (442 nm laser, 0.01 M H₂O₂ in CH₃CN, 313 K) show features corresponding to ν(M-O₂) on Ti-BEA and Nb-BEA (600-650 cm⁻¹) and ν(M=O) on Mo-BEA and W-BEA (875-980 cm⁻¹) which suggest groups 4 and 5 metals activate H₂O₂ to form peroxo (M-O₂) species and group 6 metals form oxo (M=O) species² (Figure 1b). The differences in the forms of these reactive oxygen species are likely responsible for the types of oxidation reactions that prevail on these active sites. M=O species are known to activate C-H bonds and form alcohol groups by the oxygen rebound mechanism, which involves reduction and oxidation of the active metal site³. High oxidation states and facile reduction of groups 6 metal oxide lead to surmountable barriers for this pathway and explain the formation of allylic alcohols, which lead to the enone⁴. Diols can form by hydrolysis of the primary epoxide product at acidic M-OH sites, which agrees with measured selectivity trends. These observations and interpretations provide a foundation for understanding how H₂O₂ modifies the M-BEA surface and the role of early transition M-OOH, M-O₂, and M=O reactive intermediates in epoxidations with H₂O₂.

¹ Bregante, D.T. et al. ACS Catal. 8, 2995-3010 (2018).

² Ross-Medgaarden, E. I. and Wachs, I.E. J. Phys. Chem. C. 111, 15089-15099 (2007).

³ Chen, Z. and Yin G. Chem. Soc. Rev. 44, 1083 (2015).

⁴ Kumar, A. Srinivas, D., and Ratnasamy, P. Chem. Commun., 6484-6486 (2009).

Morphological and temperature-dependent oxidative reactivity of propene thin films

Michelle Brann, Rebecca Thompson, Steven J. Sibener

Department of Chemistry
University of Chicago, Chicago, Illinois

We present results detailing the oxidative reactivity of condensed propene films with particular interest towards epoxidation product formation. These studies were conducted in a state-of-the-art ultra-high vacuum gas-surface chamber equipped for operation involving cryogenic substrate temperatures. After exposing propene films to a supersonic beam of ground state atomic oxygen, $O(^3P)$ generated from a radio frequency plasma source, RAIR spectra confirm significant propene reactivity towards a variety of products including the propylene oxide, as well as propanal and a small amount of acetone. These products differ greatly from the gas phase products (methyl and vinoxyl radicals, ethylene, and formaldehyde) since in the condensed phase, the excess energy can be dissipated by additional propene molecules on the surface so that adduct products dominate. Although the initial linear reactivity is independent of film thickness for films up to 30 ML, the amount of propanal and propylene oxide produced eventually plateaus at an amount proportional to the amount of propene starting material. Additionally, by exploring initial reaction rates at surface temperatures ranging from 44 K to 59 K, we are able to elucidate the activation energy for the reaction. Our calculated/observed activation energy ($0.5 \text{ kcal mol}^{-1}$) closely matches those reported in gas phase studies of the same system. We also note that propene crystallinity is important for reactivity as only the surface layers of amorphous propene react due to limited oxygen diffusion into the bulk film. Film composition might be able to explain slower initial rates as well as how $O(^3P)$ is unable to fully erode thicker films. Overall, this work provides fundamental mechanistic insight into the diffusion and reactivity of ground state atomic oxygen in condensed films of small, unsaturated hydrocarbons which we hope to extend to probe sterically/geometry constrained olefins reactions.

Selective detection of bacterial pathogens at single-cell resolution using metal doped carbon nanoparticles and machine learning

Maha Alafeef, Ketan Dighe, Dipanjan Pan

Bioengineering Department
University of Illinois at Urbana-Champaign, Urbana, Illinois

Rapid and accurate identification of bacterial proliferation is a critical issue in the food industry and medical diagnosis to maintain food safety and human health. To prevent the delay in therapeutic intervention, and avoid the emergence of antibiotic-resistant species; systems and devices with critical requirements such as rapid time of response, low limit of detection, ultra-sensitivity with high reproducibility and good shelf-life with robust sensing capability are needed. In this contribution, we present a novel 3D matrix sensor based on pH-sensitive fluorescent yttrium doped carbon nanoparticles (YCNPs) embedded in agarose that can rapidly and accurately detect and discriminate pathogens in real-time. The developed sensor matrix presented pH-triggered aggregation-induced emission quenching of YCNPs in a wide pH range. When the pH increased from 10.0 to 4.0, the fluorescence of the matrix decreased linearly ($R^2 = 0.9229$). The sensor's high sensitivity in a physiologically relevant pH range enables to monitor the presence of live pathogens to single-cell resolution. In addition, the 3D matrix sensor showed low cytotoxicity and long stability (>30 days). Moreover, the YCNPs platform is stable over several hours (5h) in complex medium and do not alter the bacterial growth, allowing real-time monitoring of bacterial growth with a small volume (100 μ L) and rapid response time (25 min). Furthermore, using machine learning assisted tools, different bacterial strains and blend with various cell densities was discriminated with an accuracy of 100%, thus enabling the sensor to provide fast and reliable pathogen information for clinical decisions and allow continuous monitoring of infectious disease trends.

Comparing flat-top & Gaussian femtosecond laser ablation of silicon for depth profiling in mass spectrometry

Jason Gross, Luke Hanley, Igor V. Veryovkin

Department of Chemistry
University of Illinois at Chicago, Chicago, Illinois

The optical intensity profile of a laser beam is crucial in laser micromachining and laser ablation mass spectrometry (MS). For the latter, Gaussian laser beams are usually used to probe surfaces of material and obtain two-dimensional (2D) maps of their compositions. Such 2D MS analysis can be extended into the third dimension (3D) if the probe is able to remove homogeneously thin layers of material by each laser shot. This high depth resolution of the probe is difficult to achieve with Gaussian beams because they cannot produce flat bottoms of ablated craters and can lead to artifacts in the corresponding mass spectra. To better understand laser ablation MS experiments aimed at enabling and optimizing this capability, studies of laser ablation of silicon under ambient conditions with flat-top and Gaussian beams generated by a femtosecond 800 nm laser with increasing incidence angles and numbers of laser shots were conducted. The resultant craters were characterized via optical 3D microscopy. When the beam profile was flat-top, obtained via a redistribution of photons from the most densely populated central portion of a TEM₀₀ Gaussian beam towards the “wings” for a more uniform fluence, the ablation rate was homogenized over the laser beam spot so that flat crater bottoms were achieved over a wide range of incidence angles. This enables 3D MS analysis with laser ablation probes, with ablation rates approaching <1 nm per shot, significantly steeper crater walls and minimal surface damage in comparison to the Gaussian craters. Flat bottom near-cylindrical and “splash-like” conical crater geometries observed in these experiments indicate that ablation regimes for the flat-top and Gaussian profiles, respectively, were different despite using similar laser energies. These experiments will be extended to diamond-like carbon and sapphire and will also be performed under vacuum conditions, which is relevant to depth profiling with laser ablation MS.

Solvents facilitate proton-electron transfer during the direct synthesis of H₂O₂ on Pd

Jason Adams,¹ Ashwin Chemburkar,² Yubing Lu,³ Ayman Karim,³ Matthew Neurock,² David Flaherty¹

¹University of Illinois at Urbana-Champaign, Urbana, Illinois

²University of Minnesota, Minneapolis, Minnesota

³Virginia Polytechnic Institute and State University, Blacksburg, Virginia

H₂O₂ is a benign oxidant used in alkene epoxidations and waste water treatment but is limited by high costs of the anthraquinone auto-oxidation (AO) process.¹ Direct synthesis (DS) of H₂O₂ from H₂ and O₂ may replace AO as an economical alternative if more selective catalysts are designed. Langmuir-Hinshelwood (LH) models have been proposed for this chemistry,² yet new findings suggest that H₂O₂ forms by H⁺ transfer instead.³ Such results relate to the strong dependence of H₂O₂ selectivity and rates on the solvent identity (e.g. alcohols or water) suggesting the reaction mechanism differs between solvents.^{13,3} To probe these differences, steady-state rates, kinetic isotope effects, and *operando* X-ray absorption spectra (XAS) were conducted on Pd/SiO₂ catalysts prepared by strong electrostatic adsorption of Pd(NO₃)₂ and reduction at 573 K. The kinetic isotope effect values ($k_{HkD}/$) were extracted from semi-batch reactions (5 kPa H₂ and O₂, 298 K) in isotopically labeled reactants (D₂) or solvents (e.g. D₂O, CD₃OH, and CH₃OD).

In methanol, H₂O₂ formation is independent of O₂ pressure (10-600 kPa O₂), suggesting that the Pd surface saturates with O₂-derived intermediates (O₂^{*}, OOH^{*}, H₂O₂^{*}). Methanol-derived species may then react directly with O₂ to form H₂O₂ through kinetically relevant H⁺ transfer steps, exhibiting a kinetic isotope effect ($k_{CH_3OH}/k_{CH_3OD} = 1.7 \pm 0.2$). This conclusion is supported by H₂O₂ formation rates that increase linearly with H₂ pressure under similar conditions (<100 kPa H₂). Yet, rates are greater in trideuteromethanol ($k_{CH_3OH}/k_{CD_3OH} = 0.4 \pm 0.1$), indicating that methanol-derived surface species (CH₂OH^{*}) transfer H⁺ to O₂ when forming H₂O₂. This conclusion is consistent with density functional theory (DFT) calculations showing that barriers for proton electron transfer (PET) from CH₂OH^{*} are lower than LH barriers by 38 kJ mol⁻¹. The formation of such species may explain the co-formation of CH₂O with H₂O₂, implying CH₃OH acts as a sacrificial reductant. However, these species may poison the catalyst since H₂O₂ rates decay exponentially on stream and regenerate in high O₂ pressures (800 kPa). This catalytic cycle may close through reactions between H^{*} and CH₂O^{*} to reform CH₂OH^{*} and balance the apparent H₂ stoichiometry explaining the differences in rate between H₂ and D₂ reductants ($k_{H_2}/k_{D_2} = 5.7 \pm 0.8$).

Water, in contrast, facilitates a PET mechanism analogous to the electrochemical oxygen reduction reaction (ORR). Like in methanol, the Pd likely saturates with O₂-derived intermediates, but H⁺ transfer steps are not kinetically relevant ($k_{H_2O}/k_{D_2O} = 1.0 \pm 0.1$). Instead, the kinetically relevant step likely involves electron transfer from heterolytic oxidation of H^{*} to reduce OOH^{*}, which is consistent with lower rates in D₂ versus H₂ ($k_{H_2}/k_{D_2} = 2.7 \pm 0.4$) and the proportional dependence of H₂O₂ formation on H₂ pressure (<60 kPa). DFT comparisons indicate that enthalpy barriers for PET are 15 kJ mol⁻¹ lower than those for the LH mechanism. Further, these findings are consistent with analogous ORR measurements in D₂O and H₂O showing that H⁺ do not participate in kinetically relevant oxygen reduction on noble metals.⁴ Overall, H₂O₂ forms by H⁺ transfer steps mediated by the solvent and solvent-derived surface species in both methanol and water, but the kinetically relevant steps and surface intermediates differ.

Methanol and water also affect the phase and structure of Pd catalysts as do H₂ and O₂ pressures. Water shows a discontinuous change in selectivity from 25% to 55% above a 2:1 H₂:O₂ ratio, which is not observed in methanol. *Operando* XAS at similar conditions show that nanoparticles transform from Pd to PdH_x in water while PdH_x prevails in methanol. EXAFS modelling of these spectra confirms the presence of reactive oxygen species on Pd nanoparticles in both solvents and show Pd-C coordination indicative of organic residues in methanol. Overall, these results illustrate the multifaceted role of solvents in catalysis by participating as co-reactants and co-catalysts and influencing the phase of the Pd catalyst.

¹ C. Samanta et al., Appl. Catal. A, 350, 133 (2008)

² Lawal et al. Catal. Today, 125, 40 (2007)

³ Wilson et al. J. Am. Chem. Soc., 138, 574 (2016)

⁴ Gewirth et al. J. Phys. Lett. Soc., 7 (18), 3542 (2016)

Using reflection adsorption infrared spectroscopy to investigate the surface chemistry of furfural on Pd(111)

Robert Vincent Bavisotto, Wilfred T. Tysoe

Department of Chemistry and Biochemistry
University of Wisconsin-Milwaukee, Milwaukee, Wisconsin

Furfural has been identified as a promising renewable biomass platform with the potential to be converted into biofuels. The selective modification of furfural to its derivatives is therefore of great interest. The Reflection Adsorption Infrared Spectroscopy (RAIRS) has been utilized to study the orientation and surface chemistry as a function of temperature of furfural on clean and hydrogen pre-covered palladium (111) under ultrahigh vacuum conditions. The furfural was dosed at 90K and adsorbed to the surface. The sample was then briefly annealed to selected temperatures and quickly cooled back to 90K where spectra were collected. This poster presentation will summarize the surface chemistry of furfural and furan on a clean and hydrogen pre-dosed palladium (111) crystal.

Graphene-based sensing of oxygen transport through pulmonary membranes

Marilyn Porras-Gomez,¹ Mijung Kim,² Cecilia Leal¹

¹Department of Materials Science and Engineering

²Department of Electrical and Computer Engineering
University of Illinois at Urbana-Champaign, Urbana, Illinois

Lipid-protein complexes conform the basis of pulmonary surfactants covering the respiratory surface and mediating gas exchange in lungs. Cardiolipin is a mitochondrial lipid that is overexpressed in mammalian lungs infected by bacterial pneumonia. In this paper we fabricated a graphene-based sensor to measure oxygen permeation through pulmonary membranes. Using oxygen sensing, associated X-ray scattering, and Atomic Force Microscopy structural characterization we discovered that mammalian pulmonary membranes suffer a structural transformation induced by cardiolipin and calcium ions. Surprisingly, a series of protein-free inter-membrane contacts are formed, which can have rhombohedral symmetry. Membrane contacts, or stalks, induce a significant increase in oxygen gas permeation that can lead to an imbalance in alveoli gas exchange and gas composition in blood.

Ultra-high strength and plasticity mediated by partial dislocations and defect networks

Ruizhe Su,¹ Dajla Neffati,² Qiang Li,¹ Sichuang Xue,¹ Jaehun Cho,¹ Jin Li,¹ Jie Ding,¹ Yifan Zhang,¹ Cuncai Fan,¹ Haiyan Wang,¹ Yashashree Kulkarni,² Xinghang Zhang¹

¹ School of Materials Engineering, Purdue University, West Lafayette, Indiana

² Department of Mechanical Engineering, University of Houston, Houston, Texas

Deformation mechanisms governing the strength of nanostructured metallic multilayers have been studied extensively for various applications. In general, size effect is the most effective way to tailor the mechanical strength of multilayers. Here we report that three Cu/Co multilayer systems with identical layer thickness but different types of layer interfaces exhibit drastically different mechanical behavior. *In situ* micropillar compression tests inside a scanning electron microscope show that coherent FCC (100) and (110) Cu/Co multilayer systems have low yield strength of about 600 MPa, and prominent shear instability. In contrast, the incoherent Cu/ HCP Co multilayers show much greater yield strength, exceeding 2.4 GPa, and significant plasticity manifested by a cap on the deformed pillar. Molecular dynamics simulations reveal an unexpected interplay between pre-existing twin boundaries in Cu, stacking faults in HCP Co, and incoherent layer interfaces, which leads to partial dislocation dominated high strength, and outstanding plasticity. This study provides fresh insights for the design of strong, deformable nanocomposites by using a defect network consisting of twin boundaries, stacking faults and layer interfaces.

Quantitative biodistribution of multimodal macrophage-targeted nanocarrier probes by optical and nuclear imaging

Hongping Deng,^{1,2,3} Christian J. Konopka,³ Tzu-Wen L. Cross,⁴ Kelly S. Swanson,^{4,5} Lawrence W. Dobrucki,^{1,3} Andrew M. Smith^{1,2}

¹Department of Bioengineering

²Micro and Nanotechnology Laboratory,

³Beckman Institute for Advanced Science and Technology

⁴Division of Nutritional Sciences

⁵Department of Animal Sciences

University of Illinois at Urbana-Champaign, Urbana, Illinois

Introduction: The biodistribution and pharmacokinetics of drugs and drug carriers are commonly measured through nuclear imaging but low spatial resolution prevents determination of the cell types involved. Optical imaging and cytometry provide resolution at the single cell level, but low penetration depth and dye lability makes it impossible to evaluate distribution quantitatively *in vivo*. Here, we use multimodal nuclear-optical probes for *in vivo* imaging to connect the distribution of macromolecular drug carriers across the scale of whole organisms to cells.

Results and Discussion: We developed dextran-based probes with three different dye emission windows (615 nm, 700 nm, and 800 nm) and radioisotopes (⁶⁴Cu) (Fig. 1a). The multimodal probes efficiently targeted macrophages in visceral adipose tissue (VAT) via PET/CT and optical imaging (Fig. 1b-c). There was high correlation between *in vivo* PET and *ex vivo* gamma well counting (GWC) in both white VAT and red-colored organs (liver, spleen and heart). Only dyes with 700 nm emission displayed a good correlation with GWC in VAT, however no dyes showed strong correlation in red organs (Fig. 1d-f).

Conclusions: A good correlation between nuclear and optical imaging was demonstrated with a fluorescent dye emitting at 700 nm in targeted VAT.

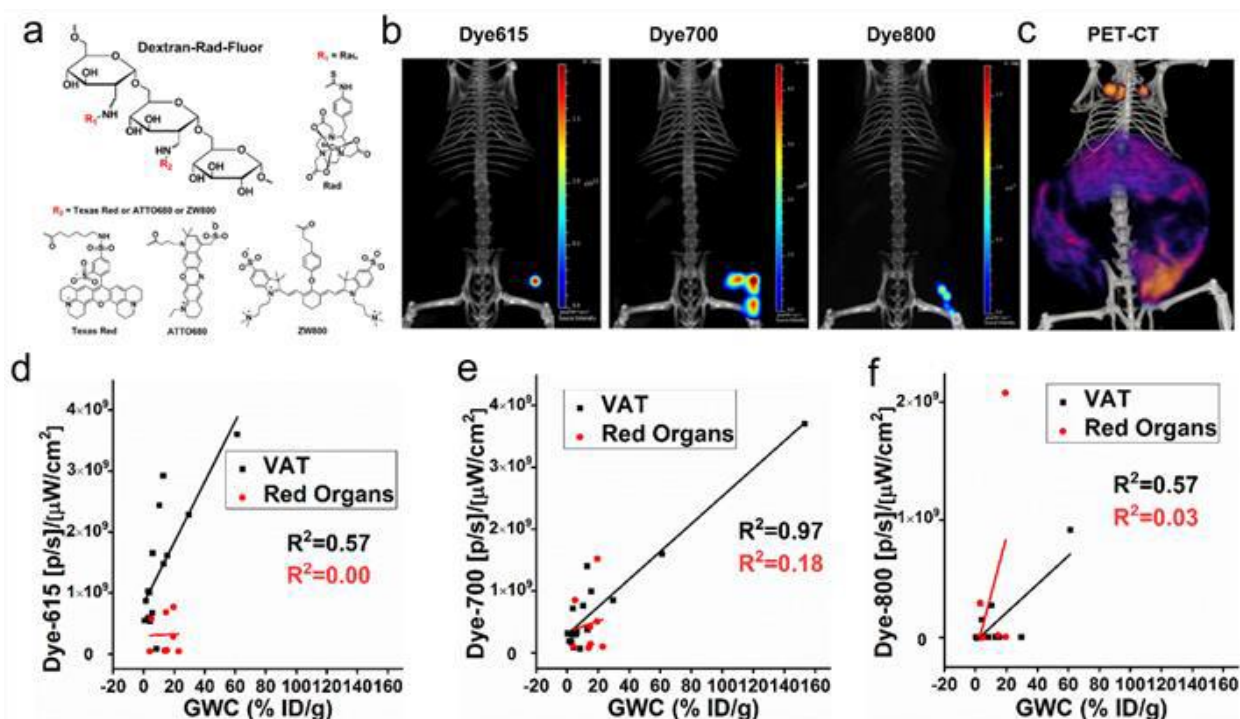


Figure 1. (a) Structures of multimodal probes. Optical (b) and reconstructed PET/CT (c) images. Correlation between nuclear and optical imaging: dye615 (d), dye700 (e) dye800 (f).

Effect of Pd isolation on the reduction of O₂ to H₂O₂ over PdAu bimetallic nanoparticles

Tomas Ricciardulli,¹ Jason S. Adams,¹ Coogan Thompson,² Ayman Karim,² David W. Flaherty¹

¹Department of Chemical and Biomolecular Engineering
University of Illinois at Urbana-Champaign, Urbana, Illinois

²Department of Chemical Engineering
Virginia Polytechnic Institute and State University, Blacksburg, Virginia

Direct synthesis of hydrogen peroxide (DS, $\text{H}_2 + \text{O}_2 \rightarrow \text{H}_2\text{O}_2$) may enable low-cost production of H₂O₂ and thus replacement of carcinogenic halogenated oxidants, which would cause a sea change in the environmental impacts of industrial selective oxidations. However, few Pd or Pt-based catalysts have been demonstrated to be sufficiently selective and stable for commercial implementation. Many groups have reported that DS selectivity may be improved by alloying Pd with Au¹, but the reason why PdAu alloys are more selective than Pd is not known.

Here, we implement an approach combining detailed kinetic analysis and orthogonal characterization techniques (FTIR of adsorbed CO, *in situ* EXAFS) to identify the cause of selectivity improvements in PdAu alloys. PdAu nanoparticles were synthesized by reduction of aqueous Pd(NO₃)₂ onto Au nanoparticles supported on silica, which were prepared by strong electrostatic adsorption of Au complexes and thermal reduction. PdAu alloys were prepared with metal contents ranging from molar Au-to-Pd ratios of 5 to 100, a wider compositional range than has been investigated so far in literature for DS. Rates for H₂O₂ and H₂O formation are independent of O₂ pressure (40-400 kPa O₂), increase in proportion to H₂ pressure below 100 kPa H₂ and become constant above 100 kPa H₂. Such trends are consistent with formation of H₂O₂ and H₂O by kinetically relevant proton-electron transfer as previously described². We observe that addition of Au to Pd results in selectivity increases and rate decreases attributable to enthalpic effects. Activation enthalpies (ΔH^\ddagger) for H₂O₂ formation increase from -3 to 19 kJ mol⁻¹ across this series of materials but are constant for catalysts with large Au (Au/Pd > 25) contents. Energetic barriers for H₂O formation, on the other hand, increase monotonically with Au content. XAS obtained *in situ* show that Pd predominantly exists as isolated monomers in the Au matrix for materials with Au/Pd ratios > 25. FTIR spectra of adsorbed ¹²CO and ¹³CO show that the distance between Pd monomers increase with catalyst Au content. Comparisons of kinetic and spectroscopic data show that the selectivity improvements in PdAu alloys are due to exploitation of differences in active site requirements for H₂O and H₂O₂ formation as H₂O₂ transition states are sensitive to the nearest Pd neighbors but agnostic to the next-nearest neighbors while H₂O formation transition states are sensitive to both nearest and next-nearest neighbors.

¹ Hutchings, et al., Phys. Chem. Chem. Phys., 2003, 5, 1917-1923

² Wilson, et al., J. Am. Chem. Soc., 2016, 138 (2), 574-586.

Nonequilibrium assembly of bottlebrush block copolymers for tunable nanoscale morphology and photonic properties through 3D solution printing

Bijal B. Patel, Dylan J. Walsh, Do Hoon Kim, Justin Kwok, Damien Guironnet, Ying Diao

Department of Chemical and Biomolecular Engineering
University of Illinois at Urbana-Champaign, Urbana, Illinois

The deliberate use of nonequilibrium processing conditions to stabilize metastable structures can dramatically affect structures formed during material self-assembly. Here we apply this principle to show systematic variation of photonic properties from thin films of a single poly(dimethylsiloxane)-*block*-poly(lactic acid) bottlebrush block copolymer. We introduce a low cost, highly versatile 3D solution printing scheme and demonstrate that by varying printing speed and substrate temperature during deposition, peak reflected wavelength for bottlebrush photonic crystals can be controlled across a range of 403 to 626 nm (blue to red). We further demonstrate the use of this technique for precise and programmable spatial patterning of photonic crystals. Via ex-situ scanning electron microscopy and synchrotron small-angle X-ray scattering analysis of printed films, we then clarify the microstructural underpinning of this phenomena: tuning of domain spacing across a range of forty nanometers. Finally, we establish the role of kinetic trapping of metastable microstructures as the driving force for domain size control based on *in situ* optical microscopy and solvent-vapor annealing experiments. This study presents a new, low cost method of functional property modulation that can be easily applied to a variety of material systems.

Investigating interactions between grafted zwitterionic polymers and proteins at nanoscale

Syeda Tajin Ahmed,¹ Deborah E. Leckband^{1,2}

¹Department of Chemical and Biomolecular Engineering

²Department of Chemistry

University of Illinois at Urbana-Champaign, Urbana, Illinois

In recent years, zwitterionic polymers have invoked a great interest among scientists for development of smart surfaces. Zwitterionic polymers have moieties possessing cationic and anionic group, which give them unique properties such as ultralow non-specific protein adsorption and biocompatibility when grafted on surface.¹ Poly(zwitterions) have been exploited where surface chemistries are important e.g. for biosensors, biomedical devices, targetable drug deliver, tissue scaffolds where binding capacity of molecular recognition elements like antibodies is challenging due to non-specific protein adsorption.^{2,3,4}

The protein-material interaction of polyzwitterions is attributed to monomer hydration, which is showed to generate both physical and energetic barriers to prevent protein binding to the polymer.^{5,6} However, there is evidence of inter-chain and intra-chain association of polyzwitterions⁷ which is a signature of their anti-polyelectrolyte behavior. In bulk solution, the presence of zwitterionic polymers have been shown to influence protein stability.⁸ Therefore, it is not well understood, why do the zwitterionic polymers interact with proteins in solution but show ultra-low fouling properties when they are grafted on substrates. Moreover, proteins are ampholytes i.e. zwitterions at their isoelectric points. Therefore, if poly (zwitterions) associate among themselves electrostatically, why would they not interact with charged and polar patches on protein surfaces? In this study, we want to test the hypothesis that the zwitterionic polymers form attractive protein-segment interactions upon penetration into the grafted chains, which depends on the relative size of the proteins and the distance between grafted chains i.e. grafting density.

Here, using polysulfobetains as model polyzwitterions, we show that, Despite known as having non-fouling qualities, grafted polysulfobetains interact with PGK (phosphoglycerate kinase) and positively charged Lysozyme proteins and the amount of adsorption of these proteins on the chains depend on the polymer configuration defined by the ratio of the distance between the grafted chain, s and the Flory radius of polymer chain in good solvent, R_F . The amount of protein adsorbed increased with increasing $s/2R_F$ i.e. with decreasing grafting density until it reaches a maximum and then starts decreasing till it reaches the amount of adsorption seen on initiator-only substrates. Here, we demonstrated that when the protein size $2R_p \ll s$, protein adsorption on grafted pSBMA chains are of ternary nature and the magnitude of adsorption can be tuned with increasing ionic strength, which has important implication in use of zwitterionic polymers to create non-fouling surfaces in different environment.

¹ Zhang Z., Chen S., Chang Y. and Jiang S. J. Phys. Chem. B 2006, 110, 10799-10804.

² Yang, W.; Bai, T.; Carr, L. R.; Keefe, A. J.; Xu, J.; Xue, H.; Irvin, C. A.; Chen, S.; Wang, J.; Jiang, S. The Effect of Lightly Crosslinked Poly(carboxybetaine) Hydrogel Coating on the Performance of Sensors in Whole Blood. Biomaterials 2012, 33, 7945-7951.

³ Limpoco, F. T.; Bailey, R. C. Real-Time Monitoring of Surface-Initiated Atom Transfer Radical Polymerization Using Silicon Photonic Microring Resonators: Implications for Combinatorial Screening of Polymer Brush Growth Conditions. J. Am. Chem. Soc. 2011, 133, 14864-14867.

⁴ Lalani, R.; Liu, L. Electrospun Zwitterionic Poly(Sulfobetaine Methacrylate) for Nonadherent, Superabsorbent, and Antimicrobial Wound Dressing Applications. Biomacromolecules 2012, 13, 1853-1863.

⁵ Shao, Q.; Jiang, S. Influence of Charged Groups on the Properties of Zwitterionic Moieties: A Molecular Simulation Study. J. Phys. Chem. B 2014, 118, 7630-7637.

⁶ Leng, C.; Hung, H.-C.; Sun, S.; Wang, D.; Li, Y.; Jiang, S.; Chen, Z. Probing the Surface Hydration of Nonfouling Zwitterionic and PEG Materials in Contact with Proteins. ACS Appl. Mater. Interfaces 2015, 7, 16881-16888.

⁷ Delgado JD. and Schlenoff JB. Static and Dynamic Solution Behavior of a Polyzwitterion Using a Hofmeister Salt Series Macromolecules 2017, 50, 4454-4464.

⁸ Kisley L., Serrano KA., Davis CM., Guin D., Murphy E., Gruebele M. and Leckband DE. Soluble Zwitterionic Poly(sulfobetaine) Destabilizes Proteins. Biomacromolecules. 2018, 19, 3894-3901.

Investigation of sulfur transport and thiolate decomposition on copper

Resham Rana, Wilfred T. Tysoe

Department of Chemistry and Biochemistry and Laboratory for Surface Sciences
University of Wisconsin-Milwaukee, Milwaukee, Wisconsin

In tribological systems, when two surfaces slide against each other, shearing induces chemical reactions of the adsorbed species and the formation of metastable species. Previous studies have shown that methyl thiolate species on copper surface decompose under shear to form adsorbed sulfur, which is transported into the subsurface region to form a metastable sulfide. In order to investigate the effect of the crystallinity of the copper on the rate of sulfur transport into the bulk, the surface-to-bulk kinetics were measured on copper foils that had been annealed to 500, 850 and 1020 K.

It is found that the sulfur transport rate into the subsurface region of copper depends on the annealing temperature. For low methyl thiolate coverages, the number of passes (rubbing cycles) required to transport sulfur into the bulk is less than for high methyl thiolate coverage and fewer rubbing cycles are required for samples annealed to higher temperatures to completely transport sulfur into the bulk with similar methyl thiolate coverages. During rubbing, methyl thiolate species also decompose to yield methane and C₂ hydrocarbons. The rate of thiolate decomposition is lower at higher methyl thiolate coverages, also lower on samples annealed at lower temperatures (500 K) compared to those annealed at higher temperatures (1020 K).

To probe the mechanical properties of the copper samples in the near-surface region during mechanical shearing, the copper was analyzed both inside and outside the wear track by measuring the nanohardness of 500-, 850- and 1020-K annealed copper samples. The Nix-Gao model was used to fit the hardness profile which calculates hardness H₀ values which showed a dependence both on rubbed (1.63, 1.60 and 0.72 GPa) and unrubbed (1.03, 0.80 and 0.71 GPa) copper samples treated at 500-, 850- and 1020-K respectively.

Printing flow planarized polymer backbone and induces drastic morphology transition of conjugated polymers

Kyung Sun Park, Justin J. Kwok, Ying Diao

Department of Chemical and Biochemical Engineering
University of Illinois at Urbana-Champaign, Urbana, IL

Flow-directed assembly is ubiquitous in additive manufacturing and offers untapped opportunities for modulating solid-state properties of functional materials. For printed electronics, printing flow can profoundly impact multiscale morphology and electronic properties of conjugated polymers, yet little is understood, let alone exploited. Herein, we report a surprising finding that printing flow is capable of planarizing the originally twisted polymer backbone, thereby altering liquid-crystal-mediated assembly pathways to result in highly aligned polymer thin films. We begin by simulating the multiphysical processes occurring during meniscus-guided printing. The interplay between evaporation-driven capillary flow and viscous-force-driven flow leads to the emergence of three printing regimes that can be characterized by their unique combinations of strain rate and residence time within the meniscus. In the “transition” regime featuring high strain rate and low residence time, we observe a twisted-to-planar molecular conformation change accompanied by a dramatic morphology transition from chiral, twinned domains to achiral, highly-aligned thin film morphology. The resulting higher conjugation length and backbone alignment lead to enhanced field-effect mobility and charge transport anisotropy. We further elucidate that such drastic morphology transition originates from removal of a twist-bend nematic liquid-crystal phase upon backbone planarization.

Oxidation reactions on Rh(111)

Marie E. Turano, Rachael G. Farber, Dan R. Killelea

Department of Chemistry and Biochemistry
Loyola University Chicago, Chicago, Illinois

The uptake and subsequent surface structures of oxygen on transition metal surfaces reveal much about the reactivity of the metal catalyst. On clean Rh(111) at room temperatures in ultra high vacuum (UHV), oxygen molecules (O_2) readily dissociate into two adsorbed oxygen atoms, asymptotically approaching a saturation coverage of 0.5 monolayers (ML, $1 \text{ ML} = 1.5 \times 10^{15} \text{ O atoms cm}^{-2}$). However, exposing Rh(111) to gas-phase oxygen atoms (atomic oxygen, AO) generated by thermally cracking molecular oxygen over a hot Ir filament, allows for higher oxygen coverages. In addition, oxygen not only adsorbs to the surface, but it may also penetrate into the subsurface region of the crystal. After atomic oxygen exposures at elevated temperatures, the Rh(111) surface is covered in a combination of oxides, adsorbed surface oxygen, and subsurface oxygen (O_{sub}). The coexistence of a variety of structures allows for the determination of which species is reactive to the oxidation of carbon monoxide (CO) on highly oxidized Rh(111) surfaces. Using scanning tunneling microscopy (STM), we have determined that CO oxidation occurs mainly at the interface between the metallic and oxidic surface phases on Rh(111) where the O_{sub} , upon emergence from the bulk, replenishes the surface oxygen. Once O_{sub} is depleted, CO consumes the oxide and the surface quickly degrades into the $(2 \times 2)\text{-O} + \text{CO}$ adlayer.

Angstrom scale chemical analysis of intermolecular and molecule-substrate interactions by ultrahigh vacuum tip-enhanced Raman spectroscopy

Sayantan Mahapatra, Jeremy F. Schultz, Nan Jiang

Department of Chemistry
University of Illinois at Chicago, Chicago, Illinois

Conventional spectroscopic techniques are limited by the optical diffraction limit to about half wavelength and therefore offers about 200 nm x 200 nm microscopic zone for working in the visible light range. Tip-enhanced Raman spectroscopy (TERS) emerges as an advanced analytical technique, where the plasmonically active probe is not only used to detect the tunneling current but also to interrogate the local chemical environment of surface adsorbed molecules with angstrom scale precision. In TERS, the incident laser irradiation is focused at the tip apex which excites localized surface plasmon (LSP) polaritons and causes the electromagnetic enhancement at the tip-sample junction. In this work, we report a topological and chemical analysis of two porphodilactone regioisomers (positional isomers) by scanning tunneling microscopy (STM), ultrahigh vacuum (UHV) TERS on Ag(100) with the spatial resolution down to 8 Å, which has wide range of applications in various field of surface science & nanotechnology such as regioselective catalysis reaction, chemical reactions, molecular electronics etc. We have shown, it is possible to distinguish these two structurally very similar forms with high accuracy & precision. Furthermore, these new class of porphyrinoids i.e. porphodilactones have been studied on different single crystals to probe the surface sensitive interactions. This work demonstrates, STM combined TERS is a complementary technique to characterize a system completely at angstrom scale.

Quantum interference enhancement of the spin-thermopower

Nathan Bennett, Justin Bergfield

Department of Chemistry
Illinois State University, Normal, Illinois

Heat can be directly converted into electricity via the thermoelectric effect in a device which has no moving parts and no operational carbon footprint. More efficient thermoelectric materials are highly sought after as energy harvesting materials and as way to understand how charge and heat interact with one another. In addition to charge, electrons carry a purely quantum property known as spin. Under the influence of an applied temperature difference, certain “spintronic” materials generate spin-dependent potentials useful for a host of applications. The interplay between spin and heat is described by the spin-thermopower, a quantity we calculate and analyze for a few interesting systems.

Hybrid functional surface derived from PDMS stamping

Muhammad Jahidul Hoque, Seok Kim, Nenad Miljkovic

Department of Mechanical Science and Engineering
University of Illinois at Urbana-Champaign, Urbana, Illinois

Hydrophobic-hydrophilic hybrid surfaces have potential to enhance and optimize condensation heat transfer. Recently, the optimum design of hybrid surfaces has been shown to greatly improve heat transfer performance when compared to that of pure hydrophobic or hydrophilic surfaces. However, challenges remain related to the manufacture of hybrid patterns on large area samples. In this work, a simple stamping method was developed to pattern surfaces for well-defined hydrophobic and hydrophilic regions. The reversible control of adhesion of patterned Polydimethylsiloxane (PDMS) stamps was utilized to form arrays of hydrophilic regions on hydroxyl-terminated dimethyl silicone (HTMS) hydrophobic surface. To benchmark the nucleation behavior, we utilized optical microscopy to study water vapor nucleation on different types and spatially patterned hybrid surfaces. Water condensation on the hybrid surfaces resulted in nucleation of droplets that initiated only on the hydrophilic patterns. Nucleation and growth of droplets on the patterned sites were monitored, as the temperature of the surface was lowered in controlled relative humidity conditions. The visualizations shown here represent design guidelines for the design of hybrid surfaces to study controlled droplet nucleation phenomena and to adjust droplet distribution and density for dropwise condensation heat transfer.

Intramolecular insights into adsorbate-substrate interactions by tip-enhanced Raman spectroscopy with angstrom-scale resolution

Jeremy Schultz, Sayantan Mahapatra, Linfei Li, Nan Jiang

Department of Chemistry
University of Illinois at Chicago, Chicago, Illinois

Adsorbate-substrate interactions determine the self-assembly and reaction mechanisms of organic molecules on a surface, and highly localized chemical effects can have profound consequences on the formation of nanoarchitectures. This sensitivity to highly localized chemical environments mandates an analytical technique capable of capturing chemical information with supreme spatial resolution. In this case, the tandem analytical technique of scanning tunneling microscopy (STM) tip-enhanced Raman spectroscopy (TERS) has been applied to interrogate the interactions of organic molecules with surfaces with angstrom-scale resolution. Through the combination of Ultrahigh Vacuum (UHV) STM-TERS with density functional theory (DFT) calculations we have studied and characterized the various interactions of self-assembled organic molecules on metal surfaces. Three molecules of interest to heterogeneous catalysis and photovoltaics were chosen, since their surface interactions are fundamental to the nature of their implementations in materials and devices. STM-TERS and DFT calculations were used to reveal molecular fingerprints and molecular binding configuration information spectroscopically. Through this method the location of specific vibrational modes can be defined, and subtle differences visualized with spatial resolution. Subsequently, these systems have been investigated for reaction stereoselectivity and binding configuration effects on self-assembly. Characterization with UHV-STM-TERS allowed these systems to be defined at the angstrom scale revealing their dependence on local chemical effects.

Dynamic-template-directed crystallization of 2D conjugated polymer thin films and their distinct electronic properties

Prapti Kafle¹, Fengjiao Zhang¹, Noah B. Schorr², Kai-Yu Huang¹, Joaquín Rodríguez-López², Ying Diao¹

¹Department of Chemical and Biomolecular Engineering

²Department of Chemistry

University of Illinois at Urbana-Champaign, Urbana, Illinois

Solution-processable polymeric semiconductors have received an increasing attention in the past two decades due to their wide range of potential applications in large-area, low-cost, flexible devices. In recent years, studies pertaining to 2D films of these semiconductors are gradually emerging owing to the development and wide recognition of 2D inorganic materials which exhibit incredible properties compared to their bulk counterparts. Analogous to the phenomenon observed in inorganic materials, reducing the dimension of polymer semiconductors films to 2D could potentially give rise to unique optoelectronic and mechanical properties. Moreover, the molecular level ultrathin body of the 2D conjugated polymer films can be incorporated in field effect transistors (FETs) to develop highly sensitive sensors for biologically relevant molecules. Despite their growing interest and utilization of a wide variety of solution processable methods, crystallization of these polymers into 2D films over large area still remain challenging. This is partially due to one dimensional nature of their intermolecular interactions as well as high conformational degrees of freedom of the polymer chains. Because 2D charge transport demands highly ordered 2D films, novel methods that enhance 2D polymer crystallization are needed. So far, fundamental questions of how electronic structure and charge transport properties depend on the number of molecular layers are still unclear. Methods for fabricating 2D layers with controlled morphology will lay the foundation for understanding these questions.

In this poster presentation, we present dynamic-template integrated meniscus-guided coating as a new technique to fabricate 2D films of conjugated polymers over centimeter length scale using a wide processing window. Using two different polymeric systems, DPP2T-TT and PII2T, we demonstrate enhanced 2D crystallization on dynamic template leading to highly ordered and aligned 2D layer with edge-on pi-pi stacking. This is in contrast to 1D fiber network morphology obtained on static substrates. Our results show that while static substrates favor ordering of alkyl chains in 2D films, dynamic template enhances ordering of the conjugated backbone with favorable $\pi - \pi$ interaction between the polymer backbone. As a result, charge transport was observed only in 2D films printed on dynamic template but not in monolayer films coated on solid substrates. In addition, we also observed a change in molecular packing from edge-on to bimodal when the film reaches a critical thickness of ~ 25 nm as well as an abrupt increase in J-aggregation, absorption coefficient and decrease in band gap and HOMO level until the critical thickness. This phenomenon was independent of the substrate and possibly arisen from straightened polymer backbone. Furthermore, we also observed an abrupt increase in hole mobility with film thickness reaching a maximum of $0.7 \text{ cm}^2\text{V}^{-1}\text{s}^{-1}$ near the critical thickness which further corroborates with the drastic increase backbone planarity as film thickness increases. Finally we also fabricated chemical sensors using bilayer polymer films which demonstrated ultrahigh sensitivity < 1 ppb to breath biomarkers.

Seeking superconducting $\text{Hf}_{1-x}\text{V}_x\text{B}_2$ ($x = 0.3$) by Co-flow of HfB_2 and V precursors

Kinsey L. Canova, Gregory S. Girolami, John R. Abelson

Department of Materials Science and Engineering
University of Illinois at Urbana-Champaign, Urbana, Illinois

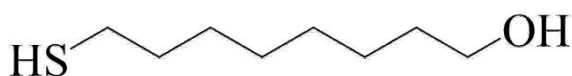
Vanadium doping in HfB_2 affords superconductivity near 5 K in the normally non-superconducting metallic ceramic HfB_2 . To deposit films of V-doped HfB_2 at low temperatures, the single-source HfB_2 precursor $\text{Hf}(\text{BH}_4)_4$ is co-flowed into the reactor with tetrakis(dimethylamido)vanadium (TDMAV). While both of these precursors have similar thermal decomposition temperatures, TDMAV, a “sticky” co-reactant often used in atomic layer deposition, produces remarkable effects in the growth kinetics of the alloy film: Growth during precursor co-flow shows a suppressed HfB_2 deposition rate which can be expressed as surface site blocking in a kinetic model. Pulsed delivery of TDMAV is explored to restore the overall growth rate and lower the vanadium concentration. The presence of a superconducting transition is surveyed by resistance measurements on the as-deposited and annealed films.

Atomic hydrogen reactions of 8-mercapto-1-octanol surfaces

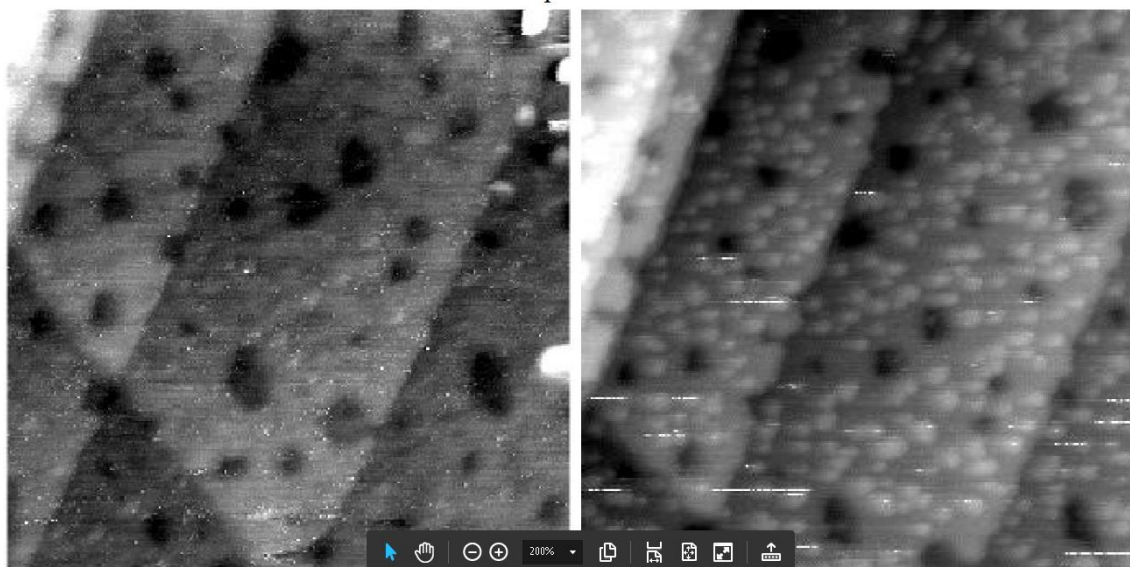
David A. Turner, Catlin N. Schalk, S. Alex Kandel

Department of Chemistry and Biochemistry
University of Notre Dame, Notre Dame, Indiana

Alkanethiolate self-assembled monolayers on Au(111) are an interesting model system for the study of gas radical reactions with organic surfaces. We use scanning tunneling microscopy (STM) to track surface changes as a result of atomic hydrogen exposure. Previous work has shown faster-than-exponential decay of an ordered 1-octanethiolate monolayer, likely due to increased reactivity at defect sites. As the chemistry of the gas-surface reaction occurs via the hydrogenation of the gold-sulfur bond, a change to the tail group would not be expected to change the rate of reaction. However, preliminary work has shown that 8-mercapto-1-octanol surfaces are disordered, unlike the 1-octanethiolate surface which has long-range ordered domains. As a consequence, functionalization of the tail group may provide a way to controllably alter the defect density and determine the effect on reaction kinetics. Initial images of the hydrogen-atom reaction with 8-mercapto-1-octanol surfaces will be presented.



8-mercapto-1-octanol



Scanning tunnelling microscopy study of alkanethiolate self-assembled monolayers and their reactivity with atomic hydrogen

Sarah Brown, Jeffrey Sayler, Steven J. Sibener

The James Franck Institute and Department of Chemistry
The University of Chicago, Chicago, Illinois

Thiolate self-assembled monolayers (SAMs) provide platforms for easily customizable organic interfaces, making them an excellent model system for studying the chemical properties of organic thin films. In particular, their reactions with atomic gas species yield important information about gas-surface interactions in organic films, specifically how static and dynamic disorder influence passivation. We are currently investigating the reactions of these SAMs with atomic hydrogen (H), using an angle-directed atomic gas source and *in situ* ultra-high vacuum scanning tunnelling microscopy (UHV-STM). First, a series of alkanethiolate samples of varying chain length (8- to 11-carbon atoms long) were reacted with H, resulting in the monolayers' conversion from close-packed standing-up phase to lower density lying-down phase. It was found that small increases in chain length caused disproportionately large decreases in reactivity at room temperature. This reaction progression was described by an exponential function with two rates: a slow rate for hydrogen reactivity with standing-up phase, which is dependent on chain length, and a fast rate for low-density phase reactions, which is the same for all samples. Chain length-dependent changes in surface morphology were also observed: short chain SAMs experienced significant etch pit reconstruction over the course of reaction, while longer chain SAMs did not. Finally, the effect of temperature on the reactivity of decanethiolate SAMs was examined by carrying out their reaction with atomic hydrogen at lower temperatures (250 K and 270 K). The SAM's reactivity was greatly reduced with decreased temperature, and reactions with H-atoms took longer than they did at room temperature. However, it was also interesting to note significant differences in the SAM's surface morphology evolution during the reaction at 250 K compared to at higher temperatures; we hypothesise that this is due to reduced thiol mobility on the Au(111) surface at this low temperature, and further investigations on this subject are ongoing.

Spectroscopic characterization of ethylidyne formed from acetylene on Pd(111)

Ravi Ranjan, Michael Trenary

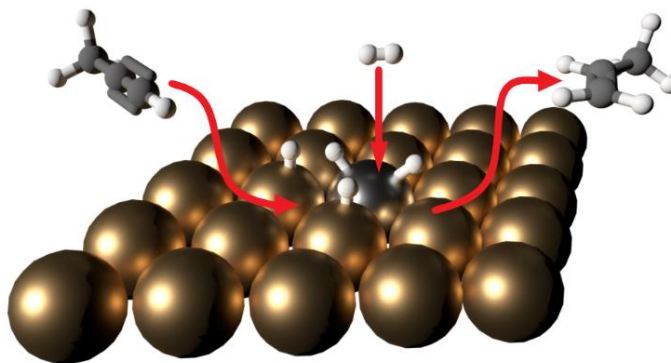
Department of Chemistry
University of Illinois at Chicago, Chicago, Illinois

The surface species formed following the adsorption and hydrogenation of acetylene (C_2H_2) on Pd(111) in the temperature range of 90-450 K are identified and characterized. The techniques used to detect the species are reflection absorption infrared spectroscopy (RAIRS) and temperature programmed desorption (TPD). Acetylene was adsorbed at low temperature and then heated to 300 K where it converts to ethylidyne (CCH_3), which is identified by its $\delta(CH_3)$ bending mode at 1327 cm^{-1} . The reaction mechanism for this conversion is quite complex; in the literature there are discrepancies in the identification of the intermediates with both vinyl ($CHCH_2$) and vinylidene (CCH_2) having been proposed. The experimental data available to date favors the formation of vinylidene as an intermediate in the conversion of acetylene to ethylidyne (CCH_3). Evidence for vinylidene is seen in the appearance of its bending mode ($\delta(HCH)$) at 1425 cm^{-1} . The possible mechanism of ethylidyne (CCH_3) formation is through isomerization of acetylene to vinylidene (CCH_2) followed by hydrogenation of vinylidene. In the temperature range of 400 to 450 K, C_2H_2 decomposes and forms a C_xH_y species as verified by TPD spectra showing an H_2 peak at 440 K following C_2H_2 adsorption at low temperature. The low energy electron diffraction (LEED) pattern of acetylene adsorbed at 95 K gives rise to a $(\sqrt{3}\times\sqrt{3})R30^\circ$ pattern. The experimental result is also supported by quantum mechanical computational calculations based on density functional theory.

Propyne hydrogenation over a Pd/Cu(111) single atom alloy catalyst studied with infrared spectroscopy

Mohammed K. Abdel-Rahman, Michael Trenary

Department of Chemistry
University of Illinois at Chicago, Chicago, Illinois



The hydrogenation of propyne (C_3H_4) to propylene (C_3H_6) using a Pd/Cu(111) single atom alloy (SAA) has been studied using polarization dependent-reflection absorption infrared spectroscopy. This method allows for simultaneous monitoring of reactants and products in the gas-phase and species adsorbed on the surface during the reaction. The results were compared with the hydrogenation of propyne using Pd-free Cu(111) as well as previous studies on Pd/Cu SAA alumina-supported metal catalysts. Propylene production first occurs at 383 K as indicated by the presence of an infrared peak at 912 cm^{-1} , which is a uniquely characteristic of gas phase propylene. The presence of propyne oligomers on the surface is indicated by a dramatic increase in the peak intensity at 2968 cm^{-1} at temperatures above 400 K. The progression of the peaks at 912 and 3322 cm^{-1} was used to calculate the rate of production of propylene and the rate of consumption of propyne, respectively. This reaction rate was used to determine a turnover frequency (TOF) for the reaction on the Pd/Cu SAA catalyst.

Interlaminar shear strength enhancement of carbon fiber composite via oxygen plasma treatment

Zhongyao Zhang,¹ Jennifer L. Wilson,² Brian R. Kitt,² David W. Flaherty¹

¹Department of Chemical and Biomolecular Engineering
University of Illinois at Urbana-Champaign, Urbana, Illinois

²Spirit AeroSystems, Inc.
Wichita, Kansas

Interlaminar shear strength is a critical factor determining mechanical performance of carbon fiber composites and influencing their applications including aerospace, automotive industry and wind energy. It is reported that interfacial properties (e.g., interfacial bonding and surface roughness) have an effect on mechanical strength of composites and surface preparation methods (e.g., abrasion and plasma treatment) have been developed for composite processing.¹ Plasma treatment is a quick and environmentally benign process to activate composite surface by changing morphology and introducing chemical functions, but it remains to be explained in detail what happens on composite surface during plasma treatment. Here, aerospace-utilized carbon fiber composite is chosen as a model material and treated by vacuum oxygen plasma, which is characterized by atomic force microscopy (AFM), surface profilometry, X-ray photoelectron spectroscopy (XPS) and fluorescence microscopy to specify the relationship between composite shear strength and interfacial properties.

The surface of carbon fiber composite (cured from Cycom 934 prepreg; Cytec Engineered Materials Inc.) was functionalized by vacuum O₂ plasma in a capacitively-coupled plasma chamber (oxygen flowrate 25 cm³ min⁻¹, pressure 220 mTorr, March CS-1701, Nordson March) with treatment time (0-8 min) and power (0-300 W) as variables. To study interlaminar shear strength of composites, FM377U (Solvay) adhesive was applied between two laminates and the composite system was cured by heat press at 450 K under a pressure of 0.69 MPa. Lap shear test (per ASTM D 3165 standard) was performed by Spirit Aerosystem lab to acquire interlaminar shear strength and plasma treated laminates (300 W, 8 min) show an increase of shear strength compared with untreated laminates (from 3500 psi to 3860 psi). Microscope pictures of fracture suggest that tested samples with larger shear strength tend to show more cohesive and substrate failure and less adhesive failure, which we proposed is influenced by both mechanical interlocking and chemical bonding at interface.

To study mechanical interlocking, surface roughness is characterized by both AFM and surface profilometry with root mean square roughness (Rq) for comparison. AFM measures Rq on a length scale of 50 μm and shows Rq increases with plasma treatment power (from 50 nm to 107 nm). Besides, surface profilometry maps an area on a length scale of 0.5 mm and Rq also increases with plasma treatment power (from 0.46 μm to 1.3 μm). Both characterizations confirm that composite surfaces become rougher after plasma treatment, which can enhance mechanical interlocking at the interface and improve interlaminar shear strength of carbon fiber composite.² Surface chemistry of carbon fiber composites is characterized by XPS and confocal fluorescence microscopy. Detailed peak fitting of N1s for composites shows an increase of feature centering around 400.6 eV (peak ratio from 17.5% to 38.1%) and this is attributed as amide or imide functions. These functions could react with epoxy groups in adhesive during curing process and form extra interfacial bonding compared with untreated composites. To confirm this hypothesis, amide or imide functions on composite surface are first hydrolyzed (1 M H₂SO₄; 24 hours; 353 K) and then probed with Texas red dye for fluorescence measurement. Preliminary results show that more dyes are grafted onto plasma treated composite surface than untreated ones, suggesting more amines are produced on plasma treated composite after hydrolysis reaction. Ongoing work seeks to establish a quantitative way for surface density of amide or imide on composite through fluorescence technique. In summary, interlaminar shear strength of carbon fiber composite is enhanced via oxygen plasma treatment, which is due to stronger mechanical interlocking and more interfacial bonding based on analysis of surface roughness and chemistry.

¹ Sharma, M.; et al. *Compos. Sci. Technol.* 2014, 102, 35-50.

² Zaldivar, R. J.; et al. *J Strain. Anal. Eng.* 2013, 49, 171-178.

Molecular self-assembly of the active pharmaceutical carbamazepine on Au(111)

Angela M. Silski, Jacob P. Petersen, Jonathan Liu, S. Alex Kandel

Department of Chemistry and Biochemistry
University of Notre Dame, South Bend, Indiana

Gaining an understanding of how the chemical design of molecular building blocks (i.e molecular geometry and type of functional groups) affects the formation of self-assembled structures in two and three dimensions, is of fundamental interest that also has implications in materials science and in the manufacture of pharmaceuticals. Carbamazepine is a highly polymorphic active pharmaceutical, and thus a good candidate for this fundamental study of polymorphism in two dimensions. In this study, self-assembled monolayers of the pharmaceutical carbamazepine and the related molecule dibenzazepine are solution-deposited on the Au(111) surface and visualized using scanning tunneling microscopy (STM). Monolayers of carbamazepine result in tetrameric clusters that are highly ordered, while a monolayer of the analog molecule in which the amide group is removed, dibenzazepine, consists of disordered clustering. Electrospray ionization mass spectra (ESI-MS) of carbamazepine shows an enhancement of a tetramer peak, which is roughly 6 times more intense than the trimer peak, indicating the anomalous stability of a 4-molecule cluster. A mass spectrum of dibenzazepine shows relatively little clustering and does not show preference for tetramers, which suggests that the amide group is crucial for the formation of the ordered tetramer networks. Our molecular modeling suggests that the carbamazepine tetramer is formed by NH-O hydrogen-bonds, with reinforcing π - π interactions between benzene rings of neighboring molecules that are responsible for the long-range order of the tetramers. The presence of an anomalously intense tetramer peak in a mass spectrum suggests that a surface is not required to support the tetramer and that the carbamazepine tetramer clusters form in solution.

Characterization of a Pd/Ag(111) single atom alloy surface using CO as a probing molecule

Mark Muir, Michael Trenary

Department of Chemistry
University of Illinois at Chicago, Chicago, Illinois

Tuning catalysts for selective hydrogenation reactions is ultimately determined by the nature of the active site for H₂ dissociation and the absorption of atomic hydrogen on the surface. Several palladium single atom alloys (SAAs) have been previously studied on different inert metals, such as Cu(111) and Au(111). In the present study, we characterize Pd/Ag(111), a new single atom alloy surface using reflection absorption infrared spectroscopy (RAIRS), temperature programmed desorption (TPD), and Auger Electron Spectroscopy (AES). CO was used as a probing molecule to determine the coordination of palladium on the Ag(111) surface. A Pd/Ag(111) surface with less than 1% palladium gave rise to a $\nu(\text{CO})$ stretching peak was seen at 2050 cm⁻¹ corresponding to CO adsorbed on palladium atoms at the on-top site, indicating a single atom alloy surface. TPD spectra gave rise to a single desorption peak was seen at 272 K corresponding to CO desorption at these sites. By increasing the palladium coverage above 1% to 13%, a second $\nu(\text{CO})$ stretching peak was seen at 1950 cm⁻¹ corresponding to CO adsorbed on palladium atoms at the bridge site, indicating palladium dimer formation. TPD spectra showed a desorption peak at 390 K, corresponding to CO desorption at these sites. By annealing these surfaces to 500 K, the palladium atoms diffuse into the subsurface, and a $\nu(\text{CO})$ stretching peak at 2150 cm⁻¹ (CO adsorbed on silver atoms) is greatly enhanced due to subsurface palladium. A 13.5% Pd/Ag(111) surface was annealed to 500 K at various time intervals and monitored before and after using RAIRS and TPD. The surface to subsurface palladium ratios were determined, and the highest SAA coverage reported was 1.5%. H₂ TPD will be investigated on these surfaces for hydrogenation reaction applications.

Biodegradable, photothermal-responsive, near-infrared fluorescent carbon dot probes for hypoxia detection

Indrajit Srivastava, Kurtis Brent, Esra Altun, Subhendu Pandit, Dipanjan Pan

Bioengineering, Materials Science and Engineering, Beckman Institute
University of Illinois at Urbana-Champaign, Urbana, Illinois
Mills Breast Cancer Institute and Carle Foundation Hospital
Urbana, Illinois

Hypoxia is a condition involving the lack of sufficient oxygen for healthy tissue metabolism. It is a characteristic amongst solid cancerous tumors. Previous techniques for hypoxia detection are highly invasive or have a limited range of depths for detection below the surface of biological tissue. In this project, we have developed a carbon dot (CD) probe that exhibits fluorescence in the near-infrared region (NIR) when exposed to a hypoxic environment. Our choice of CDs was attributed to their high photostability, high water solubility, and low cytotoxicity. NIR fluorescence emission is an important characteristic because it is the ideal range of spectrum for penetrating deeper into biological tissues. At shorter wavelengths, blood absorbs more light due to hemoglobin oxygen saturation. We have further demonstrated that these probes generate reactive oxygen species (ROS) when they are “switched” on in the NIR region, thereby making it useful for eventual photothermal ablation therapy of cancerous tumors. Finally, we have shown that these probes can be degraded by different digestive enzymes present in human body such as lipase, amylase, etc. making possibility of using these probes all the more likely.

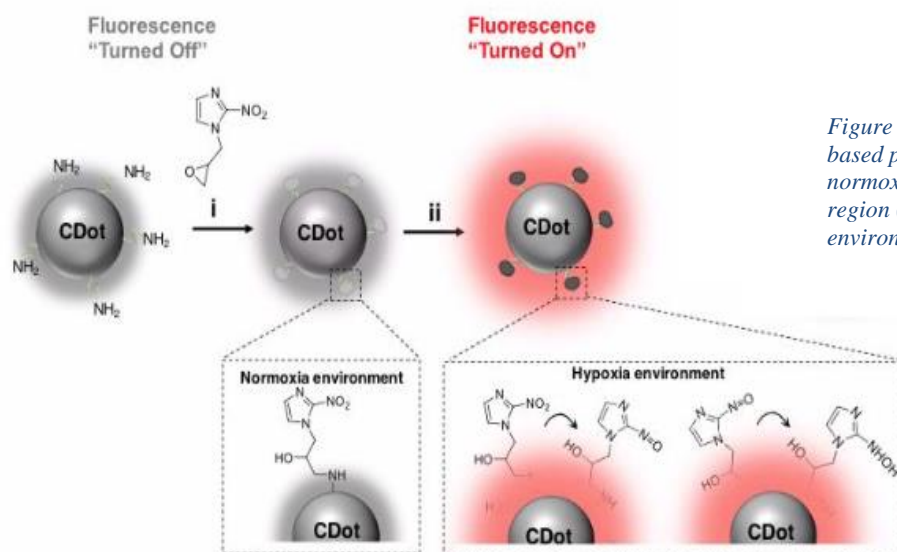


Figure 2 Scheme showing how the CDot based probe remains quenched in normoxia, but emits in the near-infrared region (NIR) once subjected to a hypoxic environment.

NanoSIMS techniques and probes for intracellular structures

Brittney L. Gorman,¹, Daphne Shen,² Mary L. Kraft,^{1,2}

¹Center for Biophysics and Computational Biology

²Department of Chemical and Biomolecular Engineering
University of Illinois at Urbana-Champaign, Urbana, Illinois

The intracellular arrangement of various lipids and proteins can vary between individual organelles as well as the plasma membrane. However, due to the small scale of cellular components probing the spatial distributions of the various components has been difficult with existing fluorescence and electron microscopy methods. High-resolution secondary ion mass spectrometry (SIMS) confers the ability to probe small structures by mapping elemental and isotopic composition with high lateral resolution and depth resolution of a few nanometers. To probe the distribution of subcellular structures, isotopically or elementally labelled components of interest are detected by rastering across the sample many times and stacking multiple image planes that show the component-specific isotopes to form a three-dimensional (3D) representation of the cell. This work uses CHO-K1 cells that stably express SNAP or Halo proteins genetically fused to organelle-specific proteins on endosomes and the Golgi apparatus, respectively. The SNAP and Halo proteins covalently react with functionalized small molecule ligands that allow detection with both fluorescence microscopy and NanoSIMS. To enhance the preservation of subcellular membranes, cells will be high-pressure frozen and fixed by freeze substitution (HPF/FS). This process upholds the previous standards for the maintenance of native distributions of proteins and lipids within the plasma membrane during freeze substitution, in addition to enhancing complex ultra-structure of internal structures that can change during fixation due to diffusion of fixatives to the subcellular structures. Labelled, fixed cells will be imaged in 3D using a Cameca NanoSIMS 50. The local abundances of isotope-labeled sphingolipids and cholesterol will be mapped in parallel with the organelle-specific labels to identify internal membranes of interest.

Magneto-optical characterization of magnetic nanoparticles in a liquid crystal matrix

Nate Fried,¹ Li Wei,¹ Maarij Syed,¹ Marissa Tousley²

¹ Department of Physics and Optical Engineering

² Department of Chemical Engineering

Rose-Hulman Institute of Technology, Terre Haute, Indiana

Magnetic measurements like Hall Effect, etc. have a long history of providing useful information related to material characterization. Here, we study iron oxide magnetic nanoparticles (MNPs) using a very sensitive AC Faraday rotation (FR) setup to show that magneto-optic techniques can be utilized to investigate magnetic response of MNPs as function of particle size, concentration, and field excitation frequency. The experimental setup employs a stabilized He-Ne laser (633 nm) along with AC magnetic field that enables lock-in detection. Iron oxide MNPs have become an area of active research given their potential as MRI contrast agents, drug carriers, and their usefulness in hyperthermia therapies. Additionally, iron oxide MNPs in liquid polymers have been investigated for possible bio applications such as novel drug delivery systems. They have been extensively studied by conventional techniques like magnetometry, TEM, small angle x-ray scattering, etc. Additionally, iron oxide MNPs in liquid polymers have been investigated for possible bio applications such as novel drug delivery systems.

While these techniques provide valuable information, they tend to be challenging, especially for liquid and gel samples. In this work we explore the organization and aggregation of MNPs in a cubic phase liquid crystal matrix. We compare these results to the behavior of the same MNPs when they are prepared in aqueous solution. We explore two different concentrations of 15 nm MNPs and 4 different magnetic field excitation frequencies. This work is meant to be an initial step in a much larger study that will explore the relationship between various phases of the liquid polymer matrix and aggregation patterns (and resulting magnetic response) of MNPs. Even at this preliminary stage, we have many interesting findings that allow us to relate the magnetic response of the samples to particle size and excitation frequency. The results provide interesting insights into the confined nature of MNP aggregates, as compared to the samples where MNPs are prepared as an aqueous solution. The experiment is conducted at room temperature and with aqueous solutions, conditions that are directly relevant to the medical applications of MNPs. We will also discuss the details of the liquid crystal matrix and future plans to explore other phases of this material.

Design, fabrication and characterization of Raman-compatible substrates that enable acquiring Raman spectra from individual cells on cell microenvironments

Isamar Pastrana-Otero, Sayani Majumdar, Aidan Gilchrist, Brendan A. C. Harley, Mary L. Kraft

Department of Chemical and Biomolecular Engineering, University of Illinois at Urbana-Champaign, Urbana, Illinois

The substrate used for the acquisition of Raman spectra from biological materials should have none-overlapping spectral signals to those from the biological materials. For this reason, Raman spectra are typically acquired from cells deposited on gold-coated substrates because gold produces minimal Raman signals that do not overlap with the spectral signature from the biological material. Unfortunately, the chemistries used to covalently attach the hydrogels that mimic cell microenvironments to the substrate were developed for glass, and glass produces a large Raman signal that overlaps the cell spectra. For compatibility with the hydrogel conjugation chemistries, while avoiding the high interfering signals produced by thick glass substrates, we fabricated custom Raman-compatible substrates in which a gold mirror is coated with a thin layer of silicate glass (SiO_2). To fabricate this Raman-compatible substrate thermal vapor deposition is used to deposit a 5 nm-thick chromium adhesion layer, which is covered with a 50 nm-thick gold layer, followed by plasma enhanced chemical vapor deposition of a 100-nm-thick SiO_2 layer. X-ray reflectivity confirmed the presence of SiO_2 and verified the thickness of deposited chrome and gold layers. Whether the custom Raman-compatible substrates enabled identifying the lineages of cells from laboratory lines with Raman spectroscopy and partial least squares-discriminant analysis (PLS-DA) was assessed by using two closely related cell lines. CHO-K1 cells and a transfected CHO-K1 (CHO-K1 T) cell line, that overexpressed an engineered protein, were seeded on functionalized soft (1 kPa) and stiff (38 kPa) hydrogels attached to the custom substrates. PLS-DA of Raman spectra acquired from individual cells on these substrates yielded a low classification error of prediction, 8.4%.

Specifically, we aim to study hematopoietic stem cell (HSC) differentiation. HSCs are responsible for hematopoiesis, the stepwise process that continuously produces all mature blood and immune cells in the body. Identifying the effects of extrinsic cues on HSC fate decisions is a necessary first step towards enabling the expansion of HSCs outside the body, for transplantation. Blood cancers that result from anomalies in hematopoiesis are treated by replacing the defective HSCs with healthy HSCs transplanted to the patient. For this purpose, we are developing a microscale platform that enables using confocal Raman microscopy to noninvasively classify individual living HSCs and their progeny according to their differentiation stages. In this platform, our Raman-compatible substrate will be covalently attached to hydrogel wells of varying stiffness that are coated with different combinations of extracellular matrix (ECM) proteins. These substrates will mimic the bone marrow microenvironment where HSCs reside. To date we assessed whether freshly isolated murine long term- HSCs (LT-HSCs) and short term- HSCs (ST-HSCs) seeded on our developed custom substrates could be accurately identified. Freshly isolated cells were seeded on functionalized soft (1 kPa) and stiff (40 kPa) hydrogels attached to the custom Raman-compatible substrates, and 16 h later, Raman spectra were acquired from 32 different cells from each population on gels with each stiffness. A PLS-DA model of this Raman spectra achieved a low classification error of prediction (9.5%). Thus, our custom Raman-compatible substrates enable accurately classifying individual living cells according to the population they belong to using PLS-DA of single-cell Raman spectra.

Structure property relationship of solid-state Li conducting network electrolyte

Naisong Shan, Chengtian Shen, Qiujie Zhao, Christopher M. Evans.

Department of Materials Science and Engineering, University of Illinois at Urbana-Champaign, Urbana, Illinois

Energy storage technology, especially at large capacity plays an important role in popularizing renewable energy, since solar, wind or hydro energy cannot be used directly. Li metal has the highest theoretical capacity as an electrode, which makes it the most ideal candidate for developing large capacity energy storage technology. However, during the operation of Li metal battery, Li dendrite can grow out of electrode surface and short the battery. The thermal runaway can ignite the organic solvent contained in the electrolyte and lead to either fire or explosion. Therefore, the dendrite growth has impeded the development of Li metal battery at a larger capacity. Ionic polymer networks are shown promising candidate for Li metal electrolytes. The covalently bonded polymer network was shown to have the ability to suppress the growth of dendrite as Li dendrite need to break the covalent bond to penetrate the electrolyte. Nevertheless, there is a lack of detailed structure-property relationship study on how network structure (crosslinking density, crosslinker length, comonomer size etc.) affecting properties (glass transition temperature (T_g), ionic conductivity etc.).

In this poster, a class of Li-conducting ionic polymer networks were precisely synthesized and engineered on a molecular level where we can tune the crosslinking density (from 1-50 mol%), the length of the crosslinker (EO3 to EO12), the Li to EO ratio (1:20 to 1:100) and the size of the comonomer (EO3 and EO6). Almost 3 orders of magnitude conductivity difference and around 70 °C T_g change were observed in the networks suggesting the network structural parameters can have a large impact on materials' properties.

Profiling individual hematopoietic cells on biomaterial-based substrates with confocal Raman micro-spectroscopy

Sayani Majumdar,¹ Isamar Pastrana-Otero,¹ Aidan Gilchrist,⁴ Brendan A. C. Harley,¹ Mary L. Kraft^{1,2,3}

¹Department of Chemical and Biomolecular Engineering,

²Department of Chemistry

³Department of Biophysics and Computational Biology

⁴Department of Materials Science and Engineering
University of Illinois at Urbana-Champaign, Urbana, Illinois

Tissue-engineering strategies to treat blood and immune diseases are predicated on our ability to expand hematopoietic stem cells (HSCs) *ex vivo*. Investigations into the complex *in vivo* microenvironment of the HSCs have revealed a host of cellular, molecular and physical stimuli that act in concert to regulate HSC behaviour and function. Miniaturized biomaterial platforms that present tens to hundreds of putative niche components can enable us to screen the effects of these cues on HSC fate in a high-throughput manner while reducing the numbers of rare cell populations required for testing. The ability to discriminate between cell populations of this lineage is crucial to this endeavor, however, conventional approaches to identify individual HSCs and their progeny are invasive and preclude longitudinal analysis of cell fate. Raman micro-spectroscopy combined with multivariate statistics is minimally invasive and quantitative and, has the potential to glean out biochemical information specific to each cell population. To study HSCs in the context of relevant physical, chemical and cellular cues using Raman micro-spectroscopy, we have developed a Raman-compatible hydrogel-based culture platform with homogeneous but tunable mechanical and biochemical properties. Three of the rarest populations of the hematopoietic hierarchy, viz. multipotent progenitor populations 1, 2 and 3 (MPP-1, MPP-2, and MPP-3, respectively) have been analyzed on hydrogel substrates presenting bone marrow-mimetic cues. The cells could be identified with >80 % accuracy, even in the presence of substrate-related spectral features. Our strategy offers an objective, reliable and label-free alternative to conventional HSC screening strategies that may be used to elucidate the extrinsic signals that drive HSCs towards specific outcomes. This knowledge may help shed more insight into the process of hematopoiesis and HSC differentiation and enable us to produce relevant hematopoietic populations for therapy.

Deformation mechanism in compressed nanocrystalline ceramic nanopillars

Haw-Wen Hsiao,¹ Shu Li,² Karin A. Dahmen,² Jian-Min Zuo¹

¹ Department of Materials Science and Engineering

² Department of Physics

University of Illinois at Urbana-Champaign, Urbana, Illinois

Nanocrystalline ceramics (NCCs) are popular as protective coating due to their exceptional mechanical properties. The high strength of NCCs derives from the effect of nanograin size, following the well-known Hall-Petch relationship. A major drawback of NCCs is their low toughness due to the limited dislocation activities. When the grain size is reduced into the nanoscale regime, the effect of grain size begins to soften materials via the increased granular activities. Such promoted activities in NCCs facilitate deformation, and thus provide a promising path to enhance the toughness of protective coatings. However, the detail of granular activities during deformation is still unclear in NCCs. It is critical to understand the underlying mechanism(s) to optimize the synthesis process and improve the mechanical properties of coatings.

The deformation mechanism of NCCs was studied by using fabricated nanopillars and in-situ compression test. Here, we report a direct observation of shear banding in nanocrystalline ZrN nanopillars. Shear banding is observed widely in a variety of materials and at different length scales. During shear banding, intense plastic shear is produced within a thin band, and shear localization strongly limits the material's ductility, leading to catastrophic failure under stress. We show that plastic deformation in ZrN is carried out by intermittent granular activities in the NCC nanopillars without brittle fracture. Localized and cooperative granular activities are found along the regions where shear bands form. Complementary cumulative distribution function (CCDF) of the associated stress drops suggests dislocation avalanches are suppressed by nanograin size.

Nanocrystalline ZrN was prepared in the form of thin film with an average grain size of 18 nm using unbalanced magnetron sputtering deposition. Nanopillars were fabricated in the plane view direction of the thin film. Compression tests of separate nanopillars were conducted in either bright-field imaging mode or nanobeam diffraction mode using Hysitron PI95 picoindenter in JEOL 2010 LaB₆ TEM. The experiments were simultaneously recorded as a video at the frame rate of 10 frames/s.

The study here demonstrates the secondary deformation mechanisms involving grain boundaries, in addition to the primary deformation mechanism operated by dislocations, and how together these mechanisms facilitate plastic deformation in nanocrystalline materials. The strong correlation of shear band formation and intermittent granular activities are demonstrated, from which a shear banding model of NCC materials is proposed.

Surface influence in the formation of supramolecular species in two dimensions

Jacob P. Petersen, A.M. Silski, S.A. Corcelli, S.A. Kandel

Department of Chemistry & Biochemistry
University of Notre Dame, Notre Dame, Indiana

Self-assembly of ferrocenecarboxylic acid on the Au(111) has been shown to produce pentamers, or five molecule clusters, which arrange in a quasicrystalline fashion. As the Au(111) surface is generally thought to be a weakly interacting surface, the role of the surface interaction in the observed structures of ferrocenecarboxylic acid was considered to be minor. However, recent results from our lab have brought this assumption into question. By altering the surface, this assumption can be tested. Two surfaces are being examined at this time; Ag(111), a chemically similar surface, and highly ordered pyrolytic graphite (HOPG), a chemically inert surface. Preliminary work has not shown signs of pentamer formation on either of these surfaces.

Photonic design of effectively transparent catalyst for higher efficiency photoelectrochemical solar fuel generators

Andrea Perry, Wen-Hui Cheng, Harry A. Atwater

California Institute of Technology, Pasadena, California

Efficient, solar-driven CO₂ reduction via a photoelectrochemical (PEC) device provides a sustainable avenue for the production of fuels typically obtained from fossil resources. Ideal device performance relies on optimal photon management to minimize losses at the device front contact while simultaneously maintaining control of the catalytic properties to achieve optimal faradaic efficiency for the CO₂ reduction reaction. We report successful fabrication of a front contact scheme using copper nanoparticles to constitute triangular grid fingers, which acts to redirect incident light to the active absorber layer of the PEC device and functions as the catalytic site for CO₂ reduction. COMSOL Multiphysics simulations of a device with 35% copper grid coverage reveal a reduction in reflection loss at the front contact by 20% with respect to bare silicon, while experimental measurements show a reduction in reflection loss by 11%. Furthermore, exposing the device to simulated AM 1.5G irradiation reveals a high photocurrent of 25 mA/cm². Dark catalysis measurements additionally demonstrate the copper's oxidation state strongly affects its faradaic efficiency towards higher-value reduction products and can be manipulated through annealing and oxidation steps. Further improvement to the device efficiency is possible via optimization of the copper triangle configuration and refinement of the fabrication procedure.

Tuning “electronic” sound through strong electron correlations

A. A. Husain,¹ M. Mitrano,¹ S. Rubeck,¹ M. Rak,¹ F. Nakamura,² C. Sow,³ Y. Maeno,³ P. Abbamonte¹

¹. Department of Physics and Seitz Materials Research Laboratory,
University of Illinois at Urbana-Champaign, Urbana, Illinois

². Department of Education and Creation Engineering
Kurume Institute of Technology, Kurume, Fukuoka, Japan

³. Department of Physics, Graduate School of Science
Kyoto University, Sakyo-ku, Kyoto, Japan

Sound is ordinarily carried in materials through vibrations of the atomic lattice, and is more or less fixed by the composition of the material. On the other hand, “electronic” sound, carried solely by valence electrons, can offer highly tunable sound velocities and propagates much faster than ordinary sound due to the difference in mass between electrons and nuclei. Electronic sound, also known quantum mechanically as the acoustic plasmon, only exists in highly two-dimensional materials or systems with a large difference in effective mass between carriers (i.e. “demons”). Fundamentally, electronic sound can be tuned by either manipulating the carrier density, or by changing the compressibility of the valence electron fluid itself. Efforts so far have focused on electrostatic gating to change the carrier density, but such an approach only works for low carrier density materials like graphene, and is impractical for metals. Here, using the homebuilt ultra-high vacuum technique of Momentum-resolved Electron Energy-Loss Spectroscopy (M-EELS), we show electronic sound in the highly two-dimensional metal Sr_2RuO_4 can be tuned by changing the electronic compressibility through its strongly temperature-dependent electron correlations. The resulting electronic sound velocity is found to change by 40% from $0.48 \text{ eV}\cdot\text{\AA}$ at 30 K to $0.67 \text{ eV}\cdot\text{\AA}$ at 300 K, and is anisotropic within the ab-plane. Our results show that strongly correlated quantum materials offer a new route for tuning electronic sound in metals, where previous approaches based on tuning carrier density are impractical.

Magneto-optical characterization of magnetic nanoparticles in aqueous solutions

Li Wei, Nate Fried, Maarij Syed

Department of Physics and Optical Engineering
Rose-Hulman Institute of Technology, Terre Haute, Indiana

Magnetic measurements like Hall Effect, etc. have a long history of providing useful information related to material characterization. Here, we study iron oxide magnetic nanoparticles (MNPs) using a very sensitive AC Faraday rotation (FR) setup to show that magneto-optic techniques can be utilized to investigate magnetic response of MNPs as function of particle size, concentration, and field excitation frequency. The experimental setup employs a stabilized He-Ne laser (633 nm) along with AC magnetic field that enables lock-in detection. Iron oxide MNPs have become an area of active research given their potential as MRI contrast agents, drug carriers, and their usefulness in hyperthermia therapies. They have been extensively studied by conventional techniques like magnetometry, TEM, etc.

While these techniques provide valuable information, they tend to be challenging, especially for liquid samples. Samples included in this study range in size from 15 nm to 25 nm. We explore two different concentrations and 4 different magnetic field excitation frequencies. This work is meant to be an initial step in a much wider ranging frequency response study that will be completed in the coming months. Even at this preliminary stage, we have many interesting findings that allow us to relate the magnetic response of the samples to particle size and excitation frequency. The experiment is conducted at room temperature and with aqueous solutions, conditions that are directly relevant to the medical applications of MNPs. We will also discuss the details of the measurement itself and its potential to be a very useful complimentary measurement to the more standard measurements mentioned above.

Impact of nanoengineered interface design on the performance of self-assembled liquid bridge confined boiling

Thomas Foulkes, Junho Oh, Nenad Miljkovic

Mechanical Science and Engineering, Electrical and Computer Engineering
University of Illinois at Urbana-Champaign, Urbana, Illinois

Increasing electrification of mechanically controlled or driven systems has created a demand for the development of compact, lightweight electronics. Removing waste heat from these high volumetric and gravimetric power dense assemblies, especially in mobile applications, requires non-traditional thermal management strategies with high heat flux potential and low integration penalty. Here, we develop and study confined subcooled pool boiling on nanoengineered interfaces which enables self-assembly of liquid bridges capable of high heat flux dissipation without external pumping. Using high speed optical imaging coupled with high-fidelity heat transfer experiments in pure vapor environments, we study the fundamental physics of liquid bridge formation, bridge lifetime, and heat transfer. We demonstrate heat flux dissipations greater than 100 W/cm^2 and heat transfer coefficients larger than $50 \text{ kW/m}^2\text{K}$ from a gallium nitride (GaN) power transistor residing above a horizontally parallel superhydrophobic nanostructured aluminum cold plate. To understand the confined bridge dynamics, we develop a hydrodynamic droplet bridging model and design rules capable of predicting the effects of gravity, intrinsic contact angle, contact angle hysteresis, and device heat flux. By demonstrating an ultra-efficient mechanism of heat dissipation and spreading using nanoengineered surfaces coupled to fluid confinement, our work enables the development of fully three-dimensional integrated electronics as well as shedding light on the fundamental physics of liquid bridging between contrasting interfaces.

Dielectric nanophotonics research involving undergraduate students at Illinois State University

Brighton Coe,¹ Daniel Eggena,¹ Andrew Missel,¹ Bailey Wilkinson,¹ Mahua Biswas,² Uttam Manna¹

¹Department of Physics
Illinois State University, Normal, Illinois
²Department of Physics and Astronomy
Millikin University, Decatur, Illinois

Resonant optical excitation of dielectric nanoparticles offers unique opportunities for future optical and nanophotonic devices because of their reduced dissipative losses and large enhancement of both the electric and magnetic nearfields. However, difficulties often arise when interpreting the observed spectra because of the overlap of the broad resonances contributed by many factors such as particle size, shape, and background index. Therefore, selective excitation of resonances that spectrally overlap with each other provides a gateway towards improved understanding of the complex interactions. In this poster, we will demonstrate selective excitation and enhancement of multipolar resonances of silicon nanospheres using cylindrical vector beams (CVBs) that we have carried out at Illinois State University.

Investigation of patterned gold nanoparticles size and spacing using block copolymer lithography

Marshall Youngblood, Mahua Biswas

Department of Physics & Astronomy
Millikin University, Decatur, Illinois

With the rise in emerging technologies in the field of optoelectronics, exploring different patterning process for plasmonic and photonic nanomaterial pattern with tunable size and spacing became imperative. In this regard, block copolymers (BCP) lithography, an inorganic nanostructure fabrication process gained significant attention due to its reproducible, large area, simple and low-cost nature. In a simple BCP lithography process, the self-assembled BCP nanostructure patterns are used as a template to infiltrate inorganic material followed by removal of the template to fabricate inorganic material nanostructure pattern. In our work, we have first deposited micelle nanostructure forming Polystyrene-block-poly (2-vinylpyridine) (PS-b-P2VP) BCPs using a spin casting method for making the template, followed by selective deposition of gold (Au) precursor into P2VP using a simple solution process method. At the end, Au nanoparticles in an orderly manner are fabricated by etching the polymers from the sample. The primary objective of this work is to investigate the size and spacing of the nanoparticle pattern by varying the average molecular weight of PS-b-P2VP molecule. We have investigated the effect of BCP deposition parameters and Au precursor deposition parameters as well. High resolution scanning electron microscopy (SEM) was used to perform physical and structural characterization of the ordered nanoparticles. These patterned Au nanoparticles of varying size and spacing will be very attractive for plasmonic applications and for induced magnetic resonance study.

In-situ Fermi level tuning of thin films during scanning tunneling microscopy studies

Yulia Maximenko, V. Humbert, Z. Wang, C. Steiner, D. Iaia, A. Aishwarya, N. Mason, V. Madhavan

Department of Physics and Materials Research Laboratory,
University of Illinois at Urbana-Champaign, Urbana, Illinois

Doping a material provides access to quantum phases such as superconductivity or the pseudo-gap phase. For a detailed atomically-resolved in-depth study of a material with a complex phase diagram, it is beneficial to implement an in-situ Fermi level tuning which can be done by back-gating. Gating is a relatively reliable technique in transport measurements, but combining it with epitaxial film growth and scanning tunneling microscopy (STM) in ultra-high vacuum (UHV) presents many technical challenges. Here, we report the design of a robust back-gating device for a versatile thin film growth and subsequent in-situ Fermi level tuning in STM. Graphene or a graphene-like material serves as the platform for the epitaxial growth, while a range of materials can be used as an insulating gate depending on the particular requirements of the experiment, including but not limited to SiO_2 , hBN, Al_2O_3 , SrTiO_3 , etc. We demonstrate successful Fermi level tuning in Bi_2Te_3 on graphene and WTe_2 on graphene in STM. The same platform also allows studying exfoliated samples as well as polymer-transferred samples.

